10:37:25 OCA PAD INITIATION - PROJECT HEADER INFORMATION 11/1[illegible]

Active

Project #: [redacted] Cost share #: Rev #: 0
Center # : R6625-0A0 Center shr #: OCA file #:
Work type : RES
Contract# [redacted] Mod #: Document : AGR
Prime #: Contract entity: GTRC

Subprojects ? : N
Main project #:

Project unit: CE Unit code: 02.010.116
Project director(s):
STURM T W CE (404)894-2218

Sponsor/division names: [redacted] /
Sponsor/division codes: 207 / 003

Award period: 881018 to 890117 (performance) 890117 (reports)

Sponsor amount	New this change	Total to date
Contract value	16,400.00	16,400.00
Funded	16,400.00	16,400.00
Cost sharing amount		0.00

Does subcontracting plan apply ?: N

Title: SANTEE-COOPER CANAL CLOSURE BY ROCKFILL, END-DUMP METHOD

PROJECT ADMINISTRATION DATA

OCA contact: Steven K. Watt 894-4820

Sponsor technical contact	Sponsor issuing office
JAMES BORG	JAMES BORG
(312)855-3323	(312)855-3323
HARZA ENGINEERING COMPANY	HARZA ENGINEERING COMPANY
150 S. WACKER DRIVE	150 S. WACKER DRIVE
CHICAGO, IL 60606	CHICAGO, IL 60606

Security class (U,C,S,TS) : U
ONR resident rep. is ACO (Y/N): N
Defense priority rating : N/A
N/A supplemental sheet
Equipment title vests with: Sponsor GIT
NONE PROPOSED

Administrative comments -
PROJECT INITIATION

12/88

GEORGIA INSTITUTE OF TECHNOLOGY
OFFICE OF CONTRACT ADMINISTRATION

NOTICE OF PROJECT CLOSEOUT

Date 5/31/89

roject No. E-20-625 Center No. R6625-0A0

roject Director T. W. Sturm School/Lab CE

ponsor Harza Engineering Co.

ontract/Grant No. Agreement dtd. 10/18/88 GTRC XX GIT ___

rime Contract No. ____________________

tle Santee-Cooper Canal Closure by Rockfill, End-Dump Method

fective Completion Date 3/20/89 (Performance) 3/20/89 (Reports)

oseout Actions Required:

- ___ None
- X Final Invoice or Copy of Last Invoice
- ___ Final Report of Inventions and/or Subcontracts
- ___ Government Property Inventory & Related Certificate
- ___ Classified Material Certificate
- ___ Release and Assignment
- ___ Other ____________________

cludes Subproject No(s). ____________________

bproject Under Main Project No. ____________________

ntinues Project No. ____________ Continued by Project No. ____________

stribution:

- Project Director
- Administrative Network
- Accounting
- Procurement/GTRI Supply Services
- Research Property Management
- Research Security Services
- X Reports Coordinator (OCA)
- X GTRC
- X Project File
- 2 Contract Support Division (OCA)
- ___ Other ____________________

Georgia Institute of Technology
A UNIT OF THE UNIVERSITY SYSTEM OF GEORGIA
ATLANTA, GEORGIA 30332

SCHOOL OF
CIVIL ENGINEERING

TELEX: 542507 GTRC OCA ATL

TELEPHONE
(404) 894-2218

March 30, 1989

Mr. James Borg, Project Manager
Harza Engineering Co.
150 South Wacker Dr.
Chicago, IL 60606

Project E20-625

Dear Jim:

Enclosed please find 10 copies of the Santee Cooper final report. I have also enclosed an extra copy of the videotape of the closure test and a complete set of 8x10 photographs that correspond to the photographic figures in the final report.

Sincerely,

Terry W. Sturm
Assoc. Prof.

c: David Bridges, GTRC

SANTEE COOPER CANAL CLOSURE BY ROCKFILL, END-DUMP METHOD

HYDRAULIC MODEL STUDY REPORT

by

Terry W. Sturm
School of Civil Engineering
Georgia Institute of Technology
Atlanta, Georgia 30332

Prepared for

HARZA ENGINEERING COMPANY
Chicago, Illinois 60606

March 1989

ACKNOWLEDGMENTS

The hydraulic model study was conducted in the Hydraulics Laboratory, School of Civil Engineering, Georgia Institute of Technology, Atlanta, Georgia for Harza Engineering Company. Graduate students Brian Dickman and Robert Hardwick made substantial contributions to both the construction and testing phases of the model study. Mr. Odis Tucker, Mechanical Technician, ably supervised the model construction. Special acknowledgment is due Mr. James Borg of Harza Engineering Company, who developed the model test procedure and managed the project.

TABLE OF CONTENTS

LIST OF FIGURES

LIST OF TABLES

1. INTRODUCTION

A hydraulic model study of the proposed emergency closure of the Santee Cooper canal by the rockfill, end-dump method was initiated by Harza Engineering Company and conducted in the Hydraulics Laboratory of the School of Civil Engineering at the Georgia Institute of Technology. The Santee Cooper Canal connects Lake Marion and Lake Moultrie, the latter of which provides water supply for the city of Charleston, South Carolina. The canal is approximately 7 miles long and has steady-state flow rates up to 25,000 cfs. It has a trapezoidal cross section with a 200-ft bottom width, side slopes of 2H:1V, and a flow depth of approximately 28 ft. The canal invert drops about two feet in elevation from approximately El. 49 ft at Lake Marion to El. 47 ft at Lake Moultrie.

In the event of failure of the dam forming Lake Marion, the Santee Cooper Canal would experience reverse flow that would drain Lake Moultrie and deprive the city of Charleston of its water supply. As a result, an emergency procedure is needed to close the canal and prevent reverse flow. Closure by the rockfill, end-dump method has been proposed. Because this closure would have to be accomplished under emergency conditions and against both a high head and flow rate, a model study with a scale of 1:40 was performed to simulate the closure procedure and to determine the size and quantity of rock needed. A pre-placed rock weir on the invert of the canal across the closure site has also been proposed, and measurements of steady-state head losses were made for this weir.

This report briefly describes the modeling laws and test procedures that were used and then summarizes the test results. Unless otherwise indicated, results are given in prototype dimensions. Overhead confetti photographs which were taken during the model closure are presented, and a videotape recording of the simulation of the canal closure accompanies this report.

2. MODEL DESCRIPTION

2.1 Modeling Laws

The canal model was constructed at a geometric scale of 1:40 as a Froude number model. The following scales must hold for dynamic similitude in a Froude number model:

$$V_r = L_r^{1/2} = 1/6.32 \quad (1)$$

$$y_r = L_r = 1/40 \quad (2)$$

$$Q_r = L_r^{5/2} = 1/10{,}119 \quad (3)$$

$$T_r = L_r^{1/2} = 1/6.32 \quad (4)$$

in which L_r=the length ratio or geometric scale=1/40; V_r=the velocity ratio; y_r=the depth ratio; Q_r=the discharge ratio; and T_r=time ratio with all ratios given as the ratio of model to prototype quantities. The steady-state tests were conducted at a prototype discharge of 25,000 cfs which corresponds to a model discharge of 2.47 cfs according to Eq. 3. Likewise, the maximum closure discharge of 43,500 cfs translates into a model discharge of 4.30 cfs. For a canal water surface elevation of 75 ft and an invert elevation of 47 ft, a canal discharge of 25,000 cfs has a prototype velocity of 3.5 ft/s and a corresponding model velocity of 0.55 ft/s with a model flow depth of 0.7 ft.

Dynamic similitude of rock movement by flowing water in a Froude number model is achieved through the use of the grain Sediment Number N_s defined by

$$N_s = \frac{V}{[(S-1)gd]^{1/2}} \qquad (5)$$

in which V=mean flow velocity or a velocity near the bed; S=specific gravity of the rock; g=gravitational acceleration; and d=grain diameter. For the model and prototype values of the Sediment Number to be equal, we must have their ratio $N_{sr}=1$. If further we have $(S-1)_r=1$ and $V_r=L_r^{1/2}$ for Froude number similarity, then $d_r=L_r$ from Eq. 5. In other words, if we use rock of the same specific gravity in model and prototype and we have a Froude number model, the grain diameter ratio is equal to the model geometric ratio of 1/40. For the Sediment Number N_s to be the sole criterion for rock movement, however, the rock diameter must be large in comparison with the thickness of the laminar sublayer. This condition was satisfied by the grain sizes used in the model.

2.2 Model Construction

The model canal was constructed inside an existing horizontal flume in the Hydraulics Laboratory of the Mason Civil Engineering Building. The flume is 80 ft long by 14 ft wide by 1.5 ft deep. An overall view of the model is shown in Fig. 1 and a construction layout of the canal inside the flume is shown in Fig. 2 in prototype dimensions.

The canal sidewalls were constructed of 3/4-in. plywood sheets which were treated with a water sealant and painted. The sidewalls were supported by inclined braces on 2-ft centers. At the toe, the sidewalls were attached and sealed to wooden toe stringers which had been sealed and anchored to the concrete floor of the flume. The floor of the canal coincided with the horizontal concrete floor of the flume.

The length of the model canal was 56 ft to give a test section with a prototype length of 2240 ft. The prototype canal cross section which was modeled had a 200 ft bottom width and a maximum depth of 40 ft with 2:1 side slopes as shown in Section A-A of Fig. 2. The centerline of the pre-placed weir was located a distance of 1120 ft downstream of the canal entrance halfway between the canal entrance and exit. The prototype length of the base of the weir was 120 ft. (All water surface profiles given in this report will use a zero longitudinal station at the entrance of the canal test section.)

Upstream of the canal entrance, inclined guidewalls were extended into the approach region to eliminate flow separation at the canal entrance. The guidewalls had a 2:1 sideslope and had a lateral offset of 1:2.5 (lateral to longitudinal) as shown in Fig. 2. Downstream of the canal exit, an exit basin was formed by the flume walls.

The flume headtank is shown in Fig. 3. Water was pumped from the laboratory sump through a 12-in. diameter pipe which was directed downward and submerged in a stilling pool formed by a 26-in. high weir. After flowing over the weir, water first passed through a wooden flow straightener, which consisted of two rows of vertical slats with 1-in. wide openings that were laterally offset, and then through a perforated steel plate with 3/8-in. diameter openings on 9/16-in. centers.

Fig. 4 shows the tailgate which was hinged about a horizontal axis at the bottom of the flume. It was raised and lowered by steel cables attached to a motor-driven shaft. Water passed over the tailgate through a bar grate back into the sump.

<u>2.3 Instrumentation</u>

A motor-driven carriage traveled on steel rails affixed to the flume and can be seen in Fig. 1. A precision point gage with a scale error in the model of ± 0.001 ft was mounted to the carriage for measuring water surface elevations. Both the lateral and longitudinal positions of the point gage could be determined from permanently attached steel tapes. The flume rail elevations were adjusted to be horizontal with an uncertainty of $\pm$0.001 ft (model) using a precision surveying level. These scale errors combined with the uncertainty in touching the flowing water surface with the point gage resulted in an estimated uncertainty in measured water surface elevations of $\pm$0.1 ft (prototype).

Water was supplied to the canal from three pumps which pump directly from the laboratory sump and are connected in parallel from the sump to a common 12-in. diameter header pipe. The flow rate is controlled by a 12-in. diameter gate valve downstream of the header pipe. The higher prototype flow rate of 43,500 cfs was produced by two identical pumps (#2 and #3) pumping together in parallel, while the lower flow rate of 25,000 cfs was supplied by pump #1 pumping alone. Each pump has its own 6-in. diameter bend meter calibrated by a large weighing tank in the Old Civil Engineering Building. In addition, the 12-in. diameter pipe which supplies the horizontal flume has an 8-in. diameter orifice meter that has been calibrated both indirectly with the bend meters and directly by the weighing tank. The standard error of estimate for these calibrations results in an uncertainty of less than one percent in the measured flow rates over the range of test discharges used in this study (10,000 to 43,500 cfs).

Overhead confetti photographs of the flow patterns through the closure dam at various stages of the closure process were taken by a camera mounted on an overhead cantilever beam. Polaroid prints and negatives were used to obtain an immediate decision on the acceptability of a particular photograph so that it could be repeated if necessary. The exposure time for the confetti photographs was one second.

2.4 Closure Rock Properties

The model rock used in the study was crushed granite supplied by Vulcan Materials of Atlanta. It had a specific gravity of 2.77 and was angular. It was supplied in standard sieve size ranges as obtained by standard sieving procedures used in the crushing plant quality control department. The sieve size ranges which were available are given in Table 1. The rock size of each rock size class d_i was calculated as the geometric mean sieve diameter.

TABLE 1.-Closure Rock Sizes

Rock	Sieve Size, in.	Geometric Mean Diameter Model, in.	Geometric Mean Diameter Prototype, ft
d1	0.5-0.75	0.61	2.0
d2	0.75-1.0	0.87	2.9
d3	1.0-1.5	1.22	4.1
d4	1.5-2.0	1.73	5.8
d5	2.0-2.5	2.24	7.4

2.5 Model Test Procedures

The steady-state head loss tests were conducted for two nominal weir heights of 5 ft and 10 ft. The pre-placed rock weir was constructed of rock d4 in Table 1 with a geometric mean diameter of 5.8 ft. The 5-ft weir consisted of one rock layer hand-placed on hardware cloth that was attached to the concrete flume floor. The 10-ft weir height was obtained by leveling off the top of the built-up rock weir with a long straight-edge set at the 10-ft height.

The steady-state test discharge of 25,000 cfs was set with the gate valve and the tailgate was adjusted to obtain the tailwater elevation indicated by the tailwater rating curve. Water surface elevations were then measured at 160 ft intervals (4 ft model) with the point gage over the 2240 ft long canal test section. The head loss tests for the 5-ft weir were conducted for tailwater elevations of 74, 75, and 76 ft, while tailwater elevations of 68, 70, 72, 74, 75, and 76 ft were used for the 10-ft weir.

The closure test procedure was devised by Harza Engineering Company based on the tailwater and headwater rating curves shown in Fig. 5 for reverse flow. The downstream control was assumed to be critical depth at Lake Marion to obtain the tailwater rating curve at the closure location. The headwater rating curve was calculated as the headwater at the closure location that would result in an assumed water surface elevation of 76.5 ft in Lake Moultrie for a given discharge. At the intersection of the two rating curves at 43,500 cfs, the headwater elevation is equal to the tailwater elevation at the closure location implying no head differential before closure starts.

Closure was begun at Q=43,500 cfs by slowly dumping 5 to 10 rocks at a time from 4-in. wide (model) shovels simultaneously on both sides of the 5-ft high pre-placed rock weir. The smallest rock d1 was used first and a rock dam was gradually built up on each side until the headwater raised no more than 1.5 ft above the rating curve or until the given rock size was no longer stable after being deposited in the flowing water. When this stage was reached, the discharge was decreased and the tailwater was adjusted according to the tailwater rating curve. Rock dumping then proceeded as before with the next larger size rock when necessary. The closure process was completed in this way by a series of placement steps as shown in Fig. 5. For a given discharge, the data points indicate the lower headwater at the beginning of rock placement and the higher headwater at the end of rock placement. This procedure approximates the actual headwater and discharge response by a sawtooth step function centered around the calculated headwater rating curve. The closure process was essentially complete after 8 placement steps.

At the end of each closure step, overhead confetti photographs of the flow through the closure dam were taken. The point gage was used to measure the boundaries of rock placement zones in the closure dam as the closure progressed.

3. MODEL RESULTS

3.1 Steady-State Head Losses

All steady-state head loss measurements were taken for a discharge of 25,000 cfs. Water surface profiles for the 5-ft weir are shown in Figs. 6 and 7 for tailwater elevations of 74, 75, and 76 ft. Figs. 6 and 7 are for two separate but identical runs that were made to determine the repeatability of the measurements. There is no apparent drop in water surface elevation due to the weir which is located between stations 1060 ft and 1180 ft. This can also be observed in Figs. 8 and 9 which show a close-up and an overall view of flow over the 5-ft weir.

The measured water surface profiles for the 10-ft weir are given for tailwater elevations of 74, 75, and 76 ft in Fig. 10 and for 68, 70, and 72 ft in Fig. 11. A dashed horizontal line is shown through the measured water surface elevations upstream of the weir to indicate the mean upstream water surface elevation. The mean upstream water surface elevation increases relative to the downstream water surface elevation as the tailwater decreases. A close-up view and an overall view of flow over the 10-ft weir are shown in Figs. 12 and 13 for a tailwater elevation of 75 ft, and in Figs. 14 and 15 for a tailwater elevation of 68 ft. The disturbance of the free surface downstream of the 10-ft weir is quite noticeable for the lower tailwater elevation of 68 ft.

Head losses were determined from the energy equation and the measured water surface elevations. The energy equation written between points 1 and 2 in the canal, taken at the canal entrance and exit, respectively, is given by

$$WS_1 + \frac{V_1^2}{2g} = WS_2 + \frac{V_2^2}{2g} + h_L \tag{6}$$

in which WS_1=upstream water surface elevation; WS_2=downstream water surface elevation; V_1=upstream velocity; V_2=downstream velocity; and h_L=total head loss. (The kinetic energy flux coefficient has been assumed to be 1.0.) Equation 6 can be used directly to calculate the head loss from measured water surface elevations, but some simplification is warranted. First, for the minimum tailwater elevation of 68 ft, the change in velocity head is a maximum and is less than 0.01 ft (prototype) and is therefore negligible. Second, the head loss term consists of both the boundary resistance loss and the minor loss due to the rock weir. The boundary resistance loss can be calculated and subtracted from the total head loss to obtain the minor loss alone. However, the maximum calculated boundary resistance head loss from water surface profile computations was found to be approximately 0.1 ft which is the same order of magnitude as the uncertainty in the water surface elevations ($\pm$0.1 ft). Therefore, to be on the conservative side, the boundary resistance head loss was not subtracted. The head loss from Eq. 6 then becomes simply the change in water surface elevation upstream of the rock weir and very far downstream of the weir. The upstream water surface elevation was taken as the mean value of the six measurements upstream of the weir and the downstream water surface elevation was taken to be the measured tailwater elevation at the canal exit. The head loss is then the difference between these two water surface elevations and is given in Table 2 for the 10 ft-weir.

TABLE 2.-Steady Flow Head Losses for 10-ft Weir; Q=25,000 cfs

Tailwater Elevation,ft	Tailwater Depth, ft	Prototype Head Loss, ft
68.0	21.0	0.76
70.0	23.0	0.47
72.0	25.0	0.35
74.0	27.0	0.16
75.0	28.0	0.09

The head loss determined for a tailwater elevation of 76 ft is too small to be reliably measured and is not included in Table 2. These head losses are plotted in Fig. 16 as a function of tailwater elevation and a best-fit curve through the data points is shown. These measurements indicate that the head loss for the 10-ft weir is no more than 0.1 ft at a tailwater elevation of 75 ft, but that it increases significantly as the tailwater drops.

In analyzing the water surface profiles for the 5-ft weir in Figs. 6 and 7, it became apparent that the head loss is less than the measurement uncertainty in the water surface elevations. Therefore all that can be concluded is that the head loss for the 5-ft weir is less than 0.1 ft for tailwater elevations of 74, 75, and 76 ft.

3.2 Closure Results

The sizes of rock used in each placement step are summarized in Table 3. Headwater elevations at the beginning and end of each placement for a given discharge are also given. These were previously shown in Fig. 5.

TABLE 3.-Headwater Elevations at Beginning and End of Each Rock Placement.

Placement No.	Q,cfs	Rock	Dia., ft	HW EL, ft Start	HW EL,ft End	TW EL, ft
1	43500	d1	2.0	74.0	75.6	73.5
2	38000	d1		74.5	75.9	71.9
3	33000	d1		74.4	75.5	70.4
4	28000	d2	2.9	73.6	76.1	68.7
5a	23000	d2		73.7	74.8	66.8
5b	23000	d3	4.1	74.8	76.8	66.8
6	18000	d3		74.4	77.1	64.8
7	13000	d3		73.6	76.7	62.4
8	10000	d4	5.8	74.0	76.5	60.8

The horizontal extent of each rock placement zone and the particular rock size used can be observed graphically in the closure dam cross section shown in Fig. 17. The final closure was completed with rock d4 with a diameter of 5.8 ft, but only a small volume of this large stone was required as shown in Fig. 17. The actual closure was stopped at 10,000 cfs when it became apparent that complete closure could be achieved by further building up the bottom of the remaining V-notch gap without further increases in stone size.

Confetti photographs at the end of each placement step are shown in Figs. 18 to 25. The upper part of each figure is a photograph of water flowing without confetti to show clearly the lateral extent of the closure dam, while the lower photograph shows the streamline pattern traced out by the confetti particles for the flow through the constriction formed by the closure dam. Flow is from left to right in each figure. The streamline patterns show very clearly the increasing curvature due to flow contraction through the notch between the two opposite closure dikes as closure progresses. In addition, the streamlines show some seepage through the rock dikes as closure progresses. A few rocks can be seen downstream. They were moved there by the flow during hand placement as the threshold of movement for a particular rock size was approached.

As a means of determining repeatability of the closure process, all rocks larger than a diameter of 2.9 ft (d2) were removed from the closure dam, and the closure process was begun again in a separate test with rock d3 and placement no. 5b. In this test it was possible to achieve complete closure with rock d3 (dia. = 4.3 ft) without using the next larger size. This result was obtained possibly because the nose of each closure dike was angled upstream more severely during the rock placement than in the previous test.

The final closure dam contours are shown in Fig. 26 and a photograph of the final closure dam can be seen as Fig. 27. There is a preponderance of the larger size rock on the upstream side of the dam near the flow centerline where the noses of the two closure dikes were brought together.

Seepage tests were run at the end of the second test and results are shown in Table 4. These results indicate a substantial amount of seepage through the rock dam.

TABLE 4.-Seepage Capacity of Rock Dam

Q, cfs	HW EL, ft	TW EL, ft
10,000	70.4	60.8
13,000	77.3	62.4

4. CONCLUSIONS

It is concluded from the steady flow head loss tests at Q=25,000 cfs that the head loss across the 5-ft weir was considerably less than 0.1 ft and was not measurable for tailwater elevations of 74, 75, and 76 ft. Head losses for Q=25,000 cfs with the 10-ft weir were approximately equal to 0.1 ft for a tailwater elevation of 75 ft and increased rapidly as the tailwater decreased reaching a value of nearly 0.8 ft for a tailwater elevation of 68 ft.

The closure test was successful. Closure was begun with a rock having a geometric mean diameter of 2.0 ft at Q=43,500 cfs, continued with rock sizes of 2.9 ft and 4.1 ft, and was completed with a relatively small volume of 5.8-ft diameter rock. The test results clearly indicate the volume of each rock size required to complete the closure. The closure process was shown to be repeatable, although a slight dependence of the final closure on the upstream angle of the nose of the closure dikes was observed. The best method for placing the rock was to gently push it over the edge of the closure dike at an upstream angle of approximately 45 degrees relative to the flow direction. A substantial seepage flow occurred through the rock dam itself.

5. APPENDIX: Figures

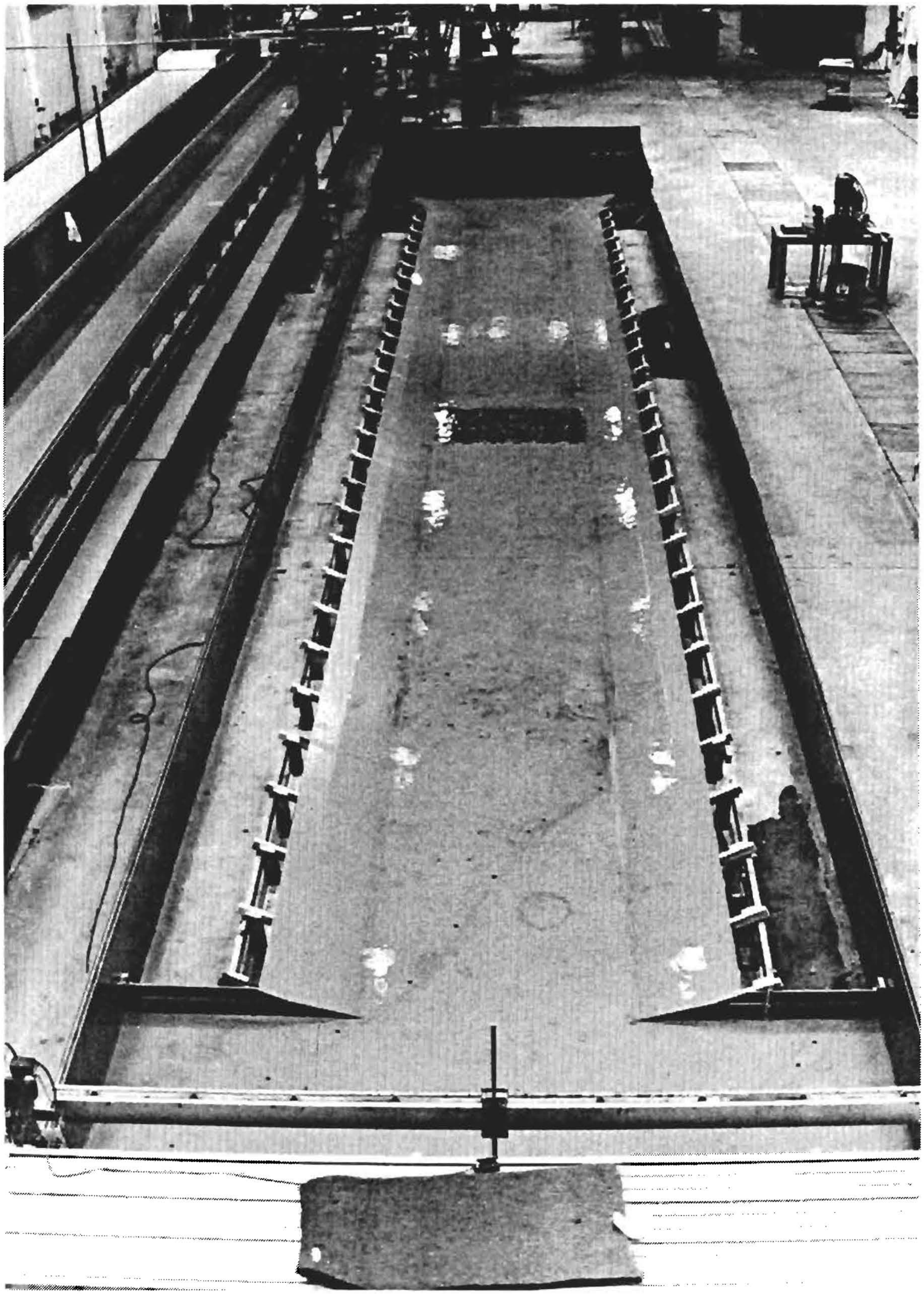

Fig. 1-Overall View of Santee Cooper Canal Model Looking Upstream

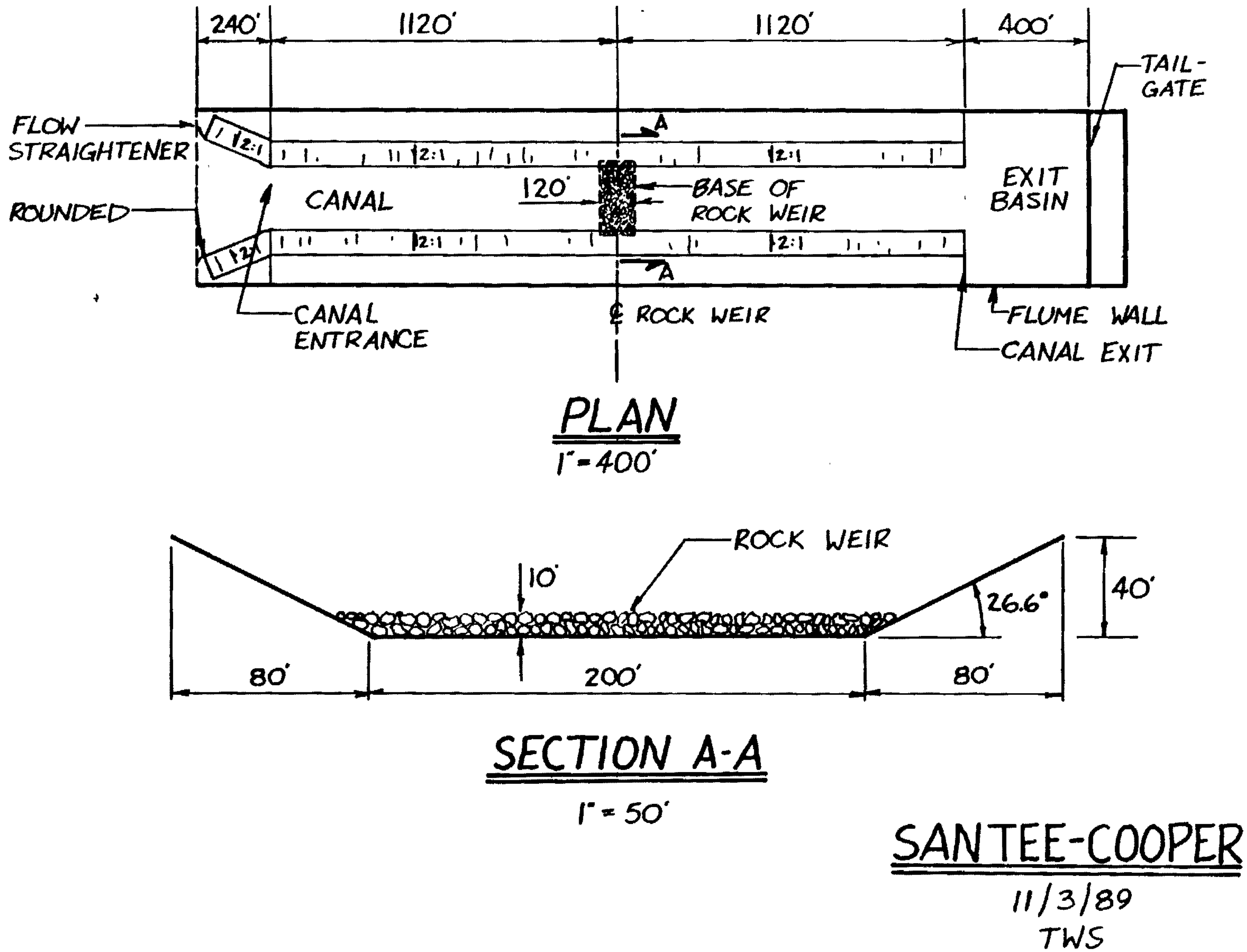

Fig. 2-Construction Layout of Santee Cooper Canal

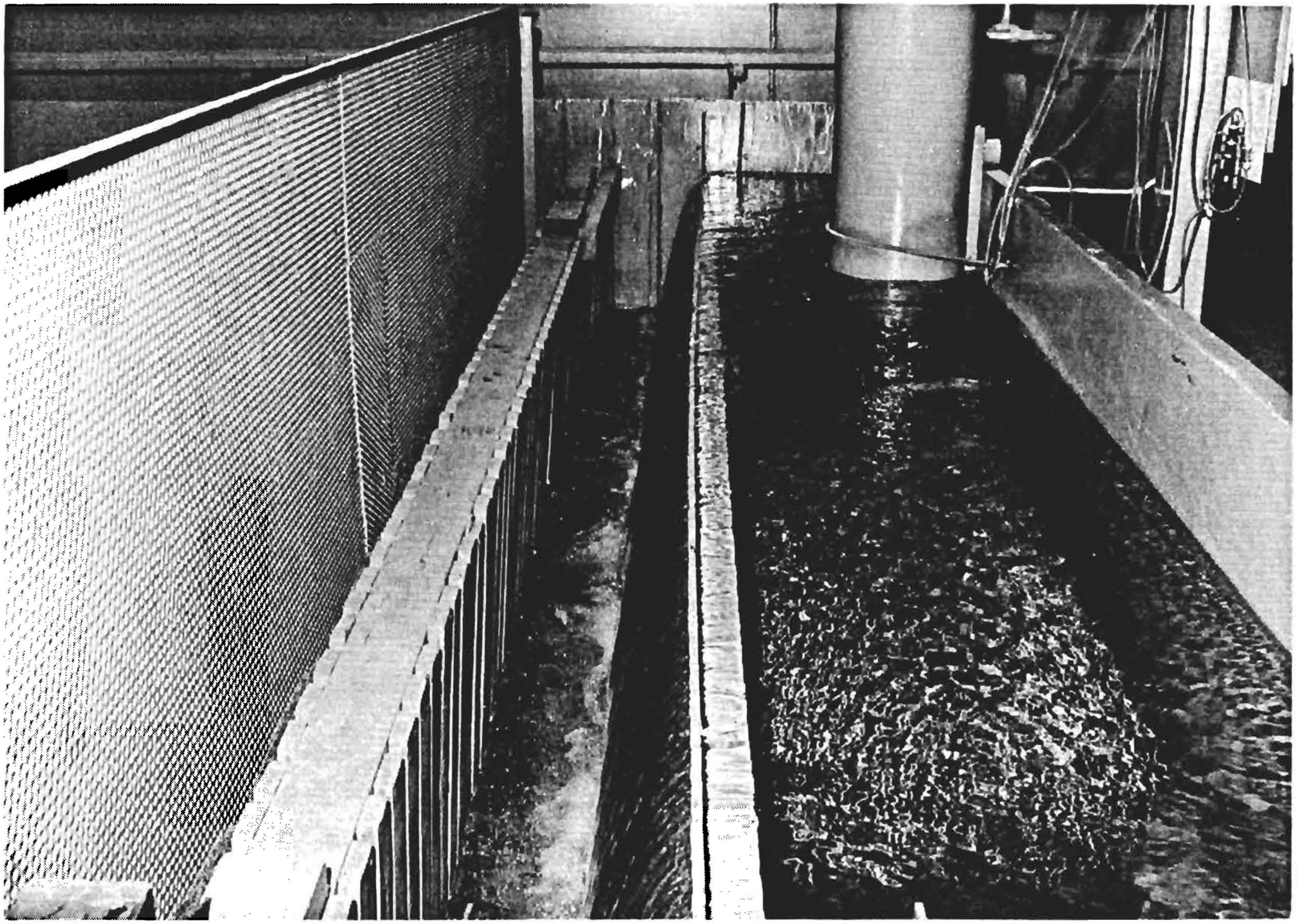

Fig. 3-Head Tank and Flow Straighteners

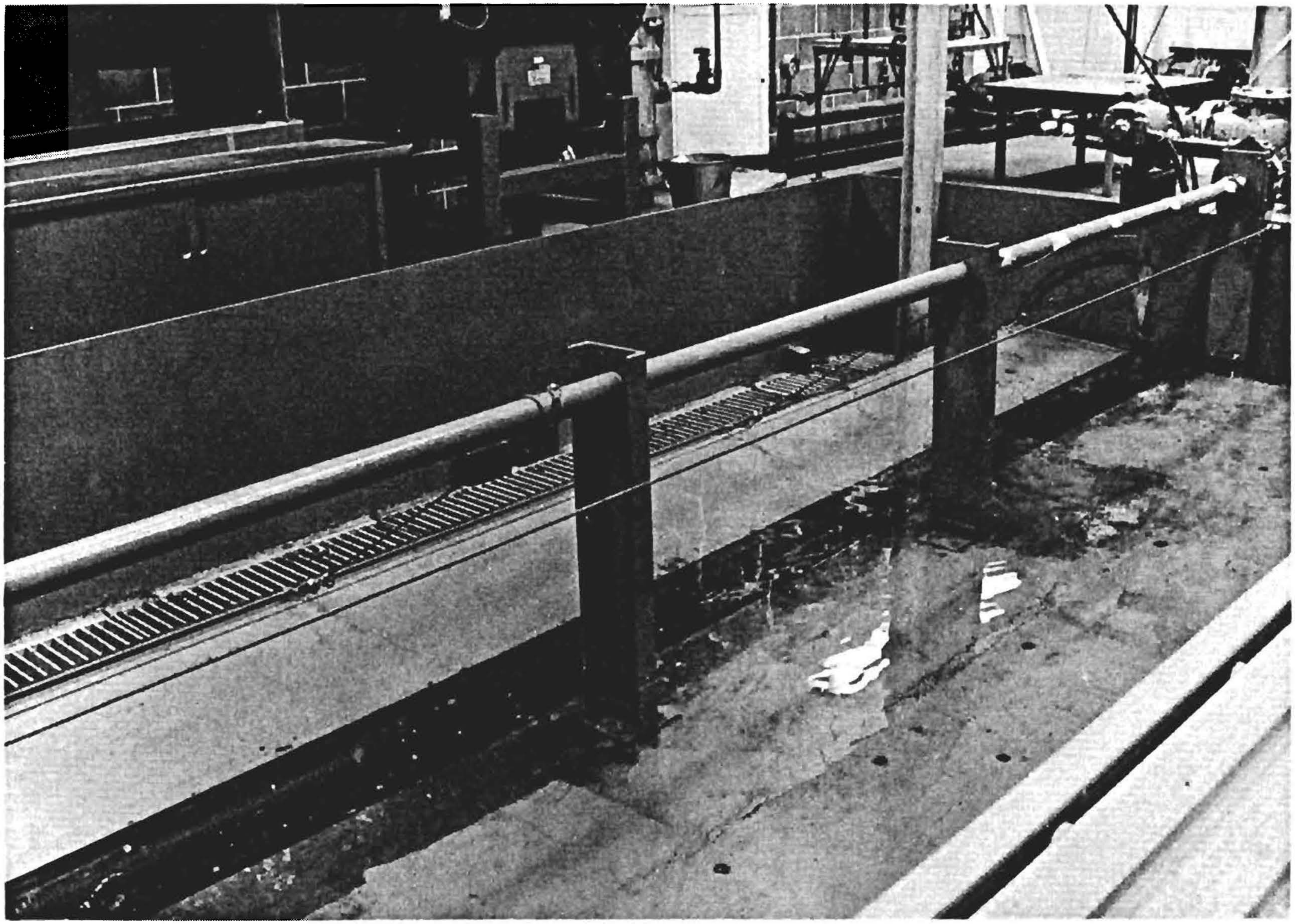

Fig. 4-Tailgate and Lifting Mechanism

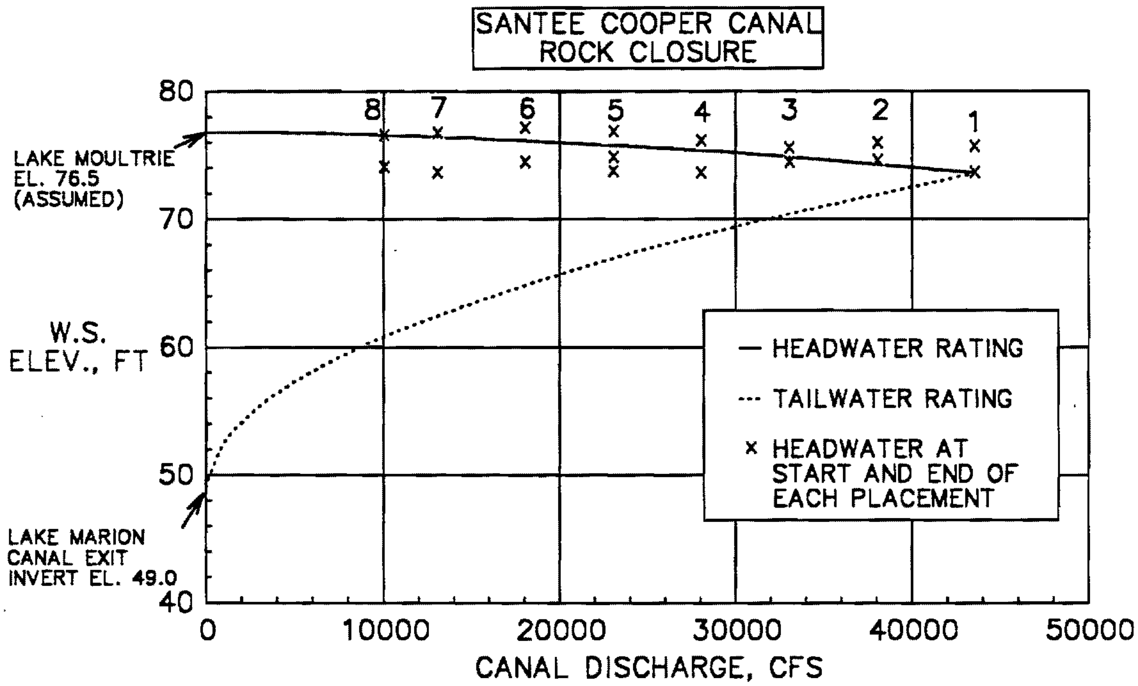

Fig. 5-Santee Cooper Canal Headwater and Tailwater Rating Curves at Closure Site and Measured Headwater at Start and End of Each Rock Placement

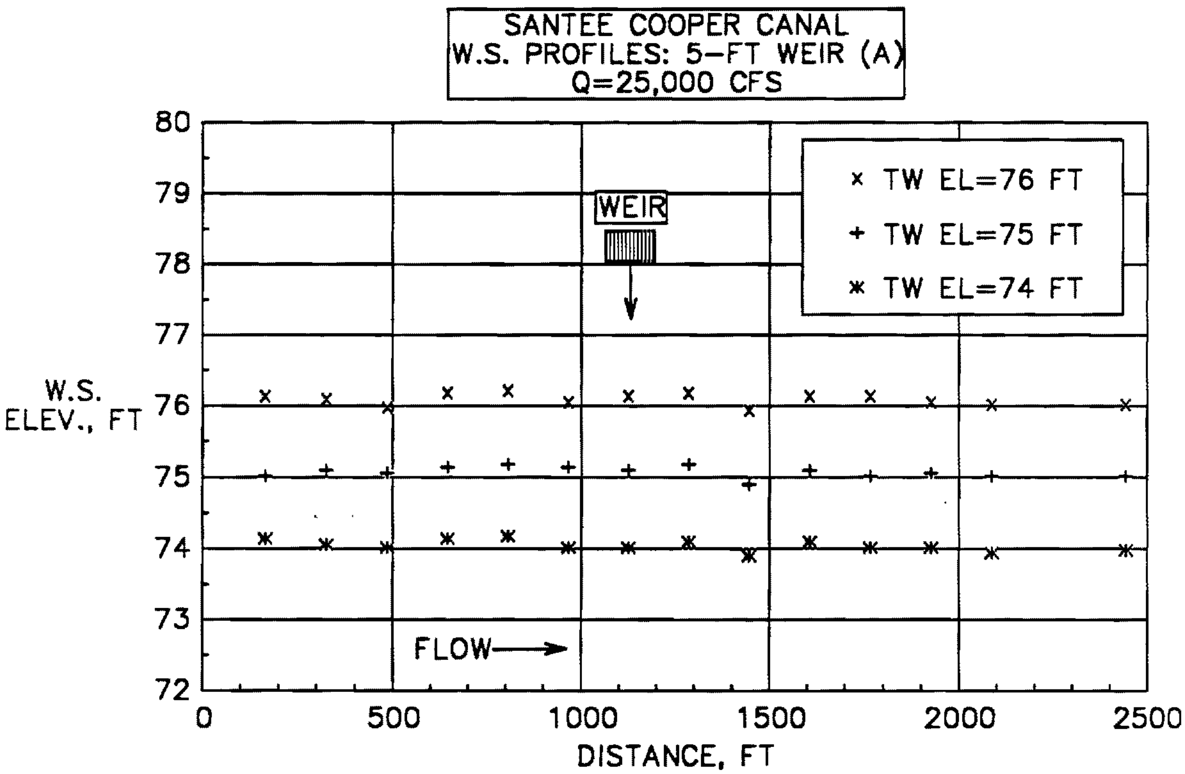

Fig. 6-Water Surface Profiles for 5-ft Weir (Run A); Q=25,000 cfs

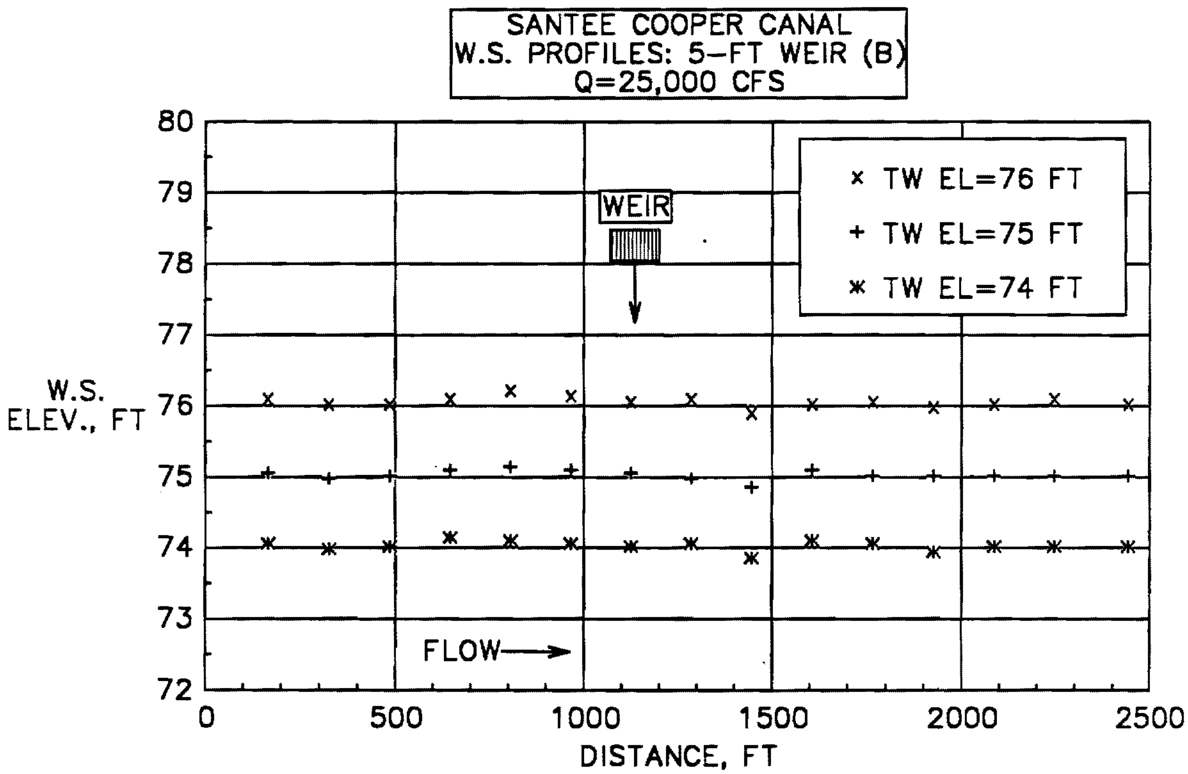

Fig. 7-Water Surface Profiles for 5-ft Weir (Run B); Q=25,000 cfs

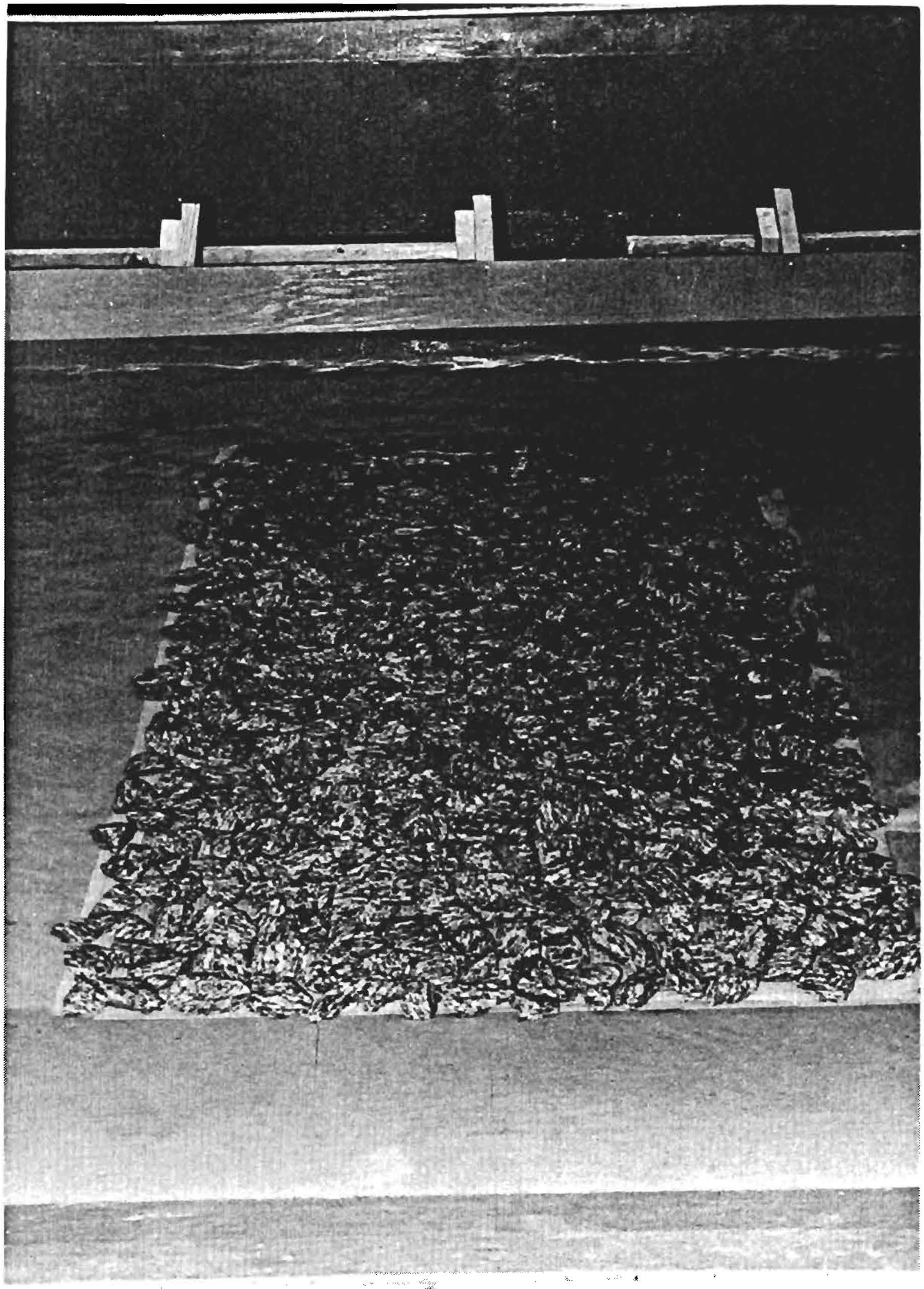

Fig. 8-Close-Up View of Flow (Right to Left) Over 5-ft Weir; Q=25,000 cfs; Tailwater Elevation=75 ft

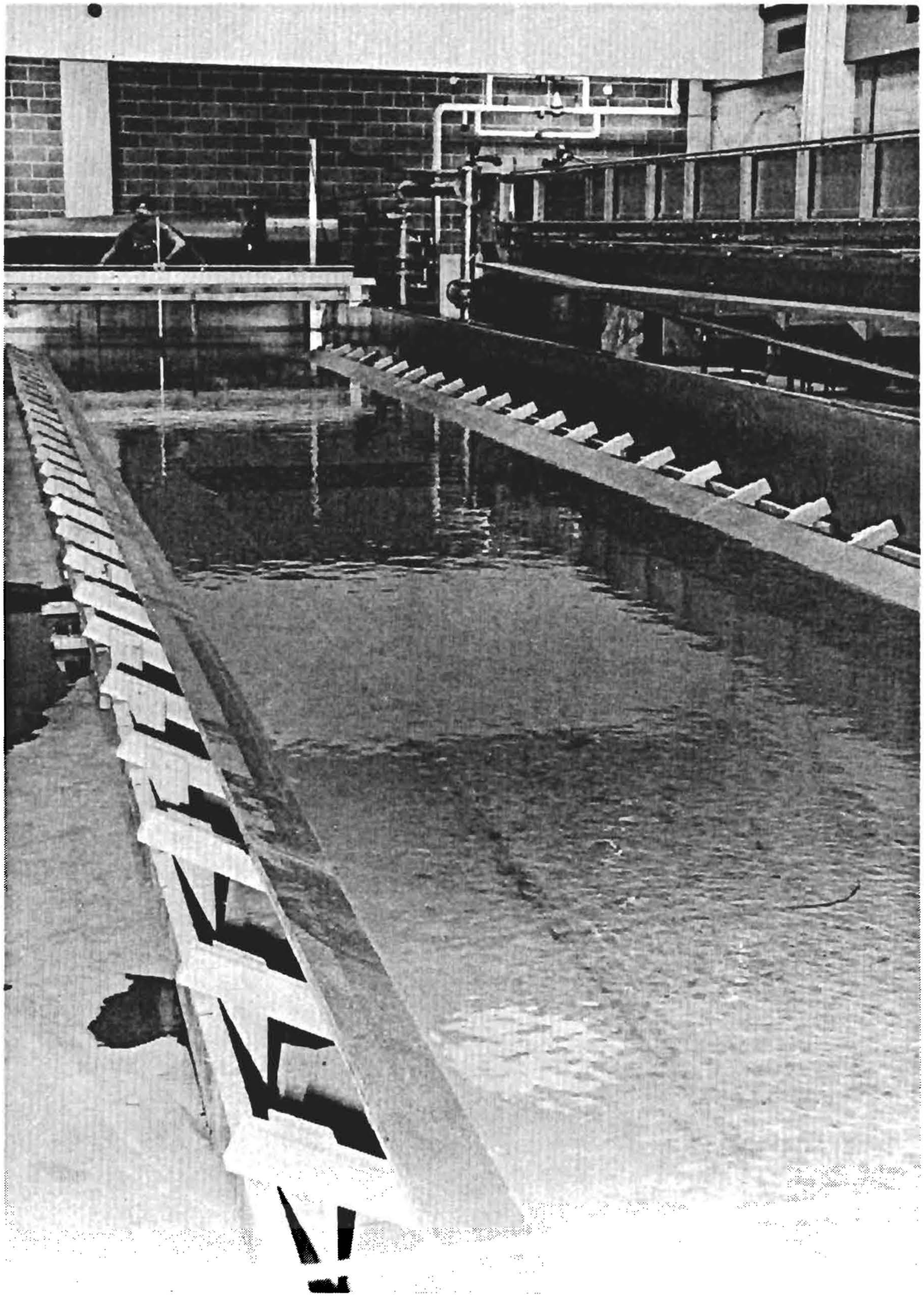

Fig. 9-Overall View of Flow Over 5-ft Weir Looking Downstream; Q=25,000 cfs; Tailwater Elevation=75 ft

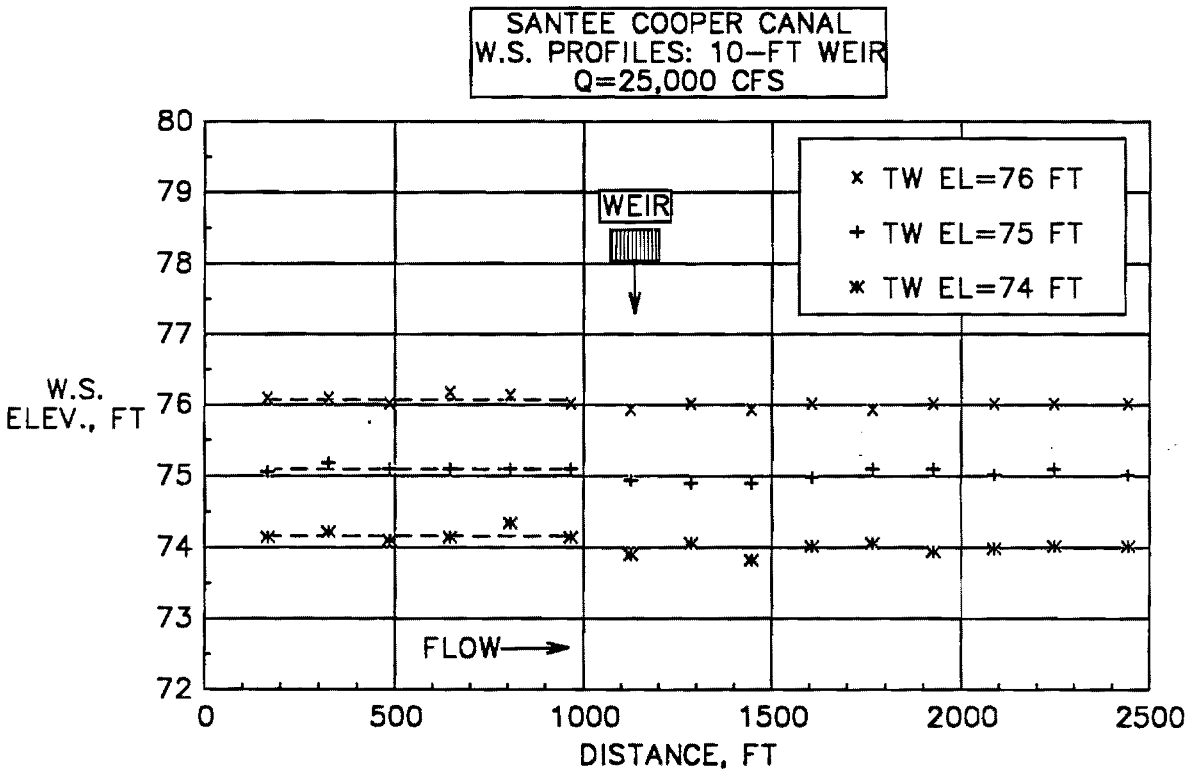

Fig. 10-Water Surface Profiles for 10-ft Weir (Run A); Q=25,000 cfs; Tailwater Elevation=74, 75, 76 ft

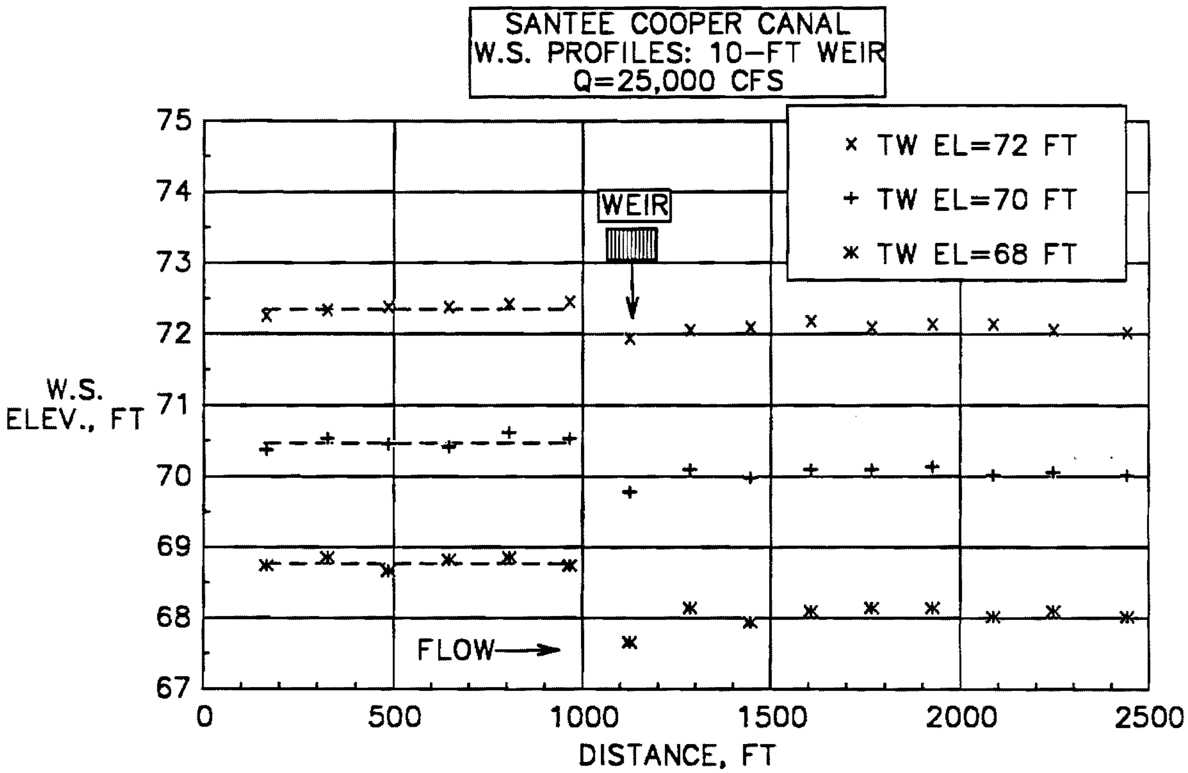

Fig. 11-Water Surface Profiles for 10-ft Weir (Run B); Q=25,000 cfs; Tailwater Elevation=68, 70, 72 ft

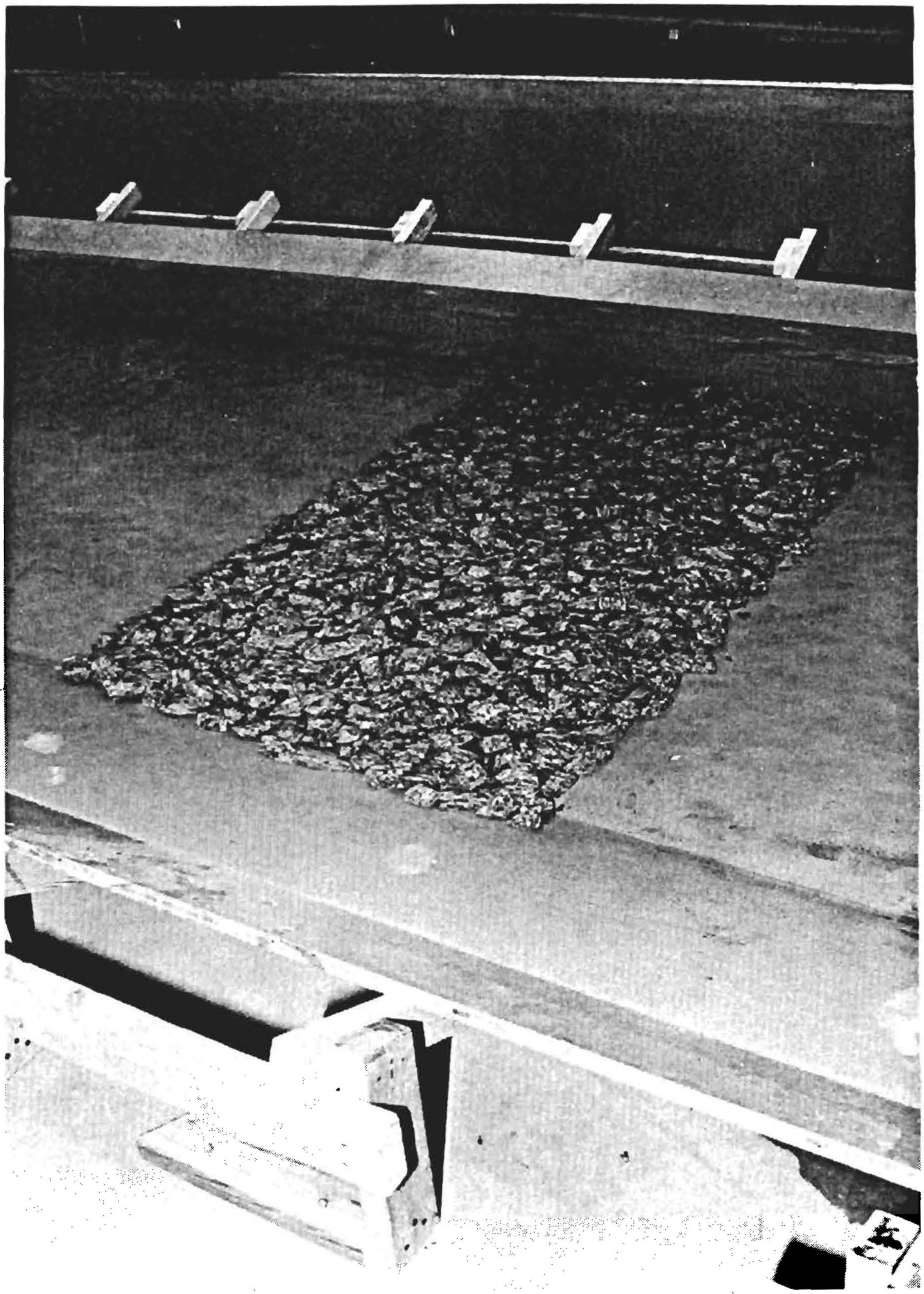

Fig. 12-Close-Up View of Flow (Right to Left) Over 10-ft Weir; Q=25,000 cfs; Tailwater Elevation=75 ft

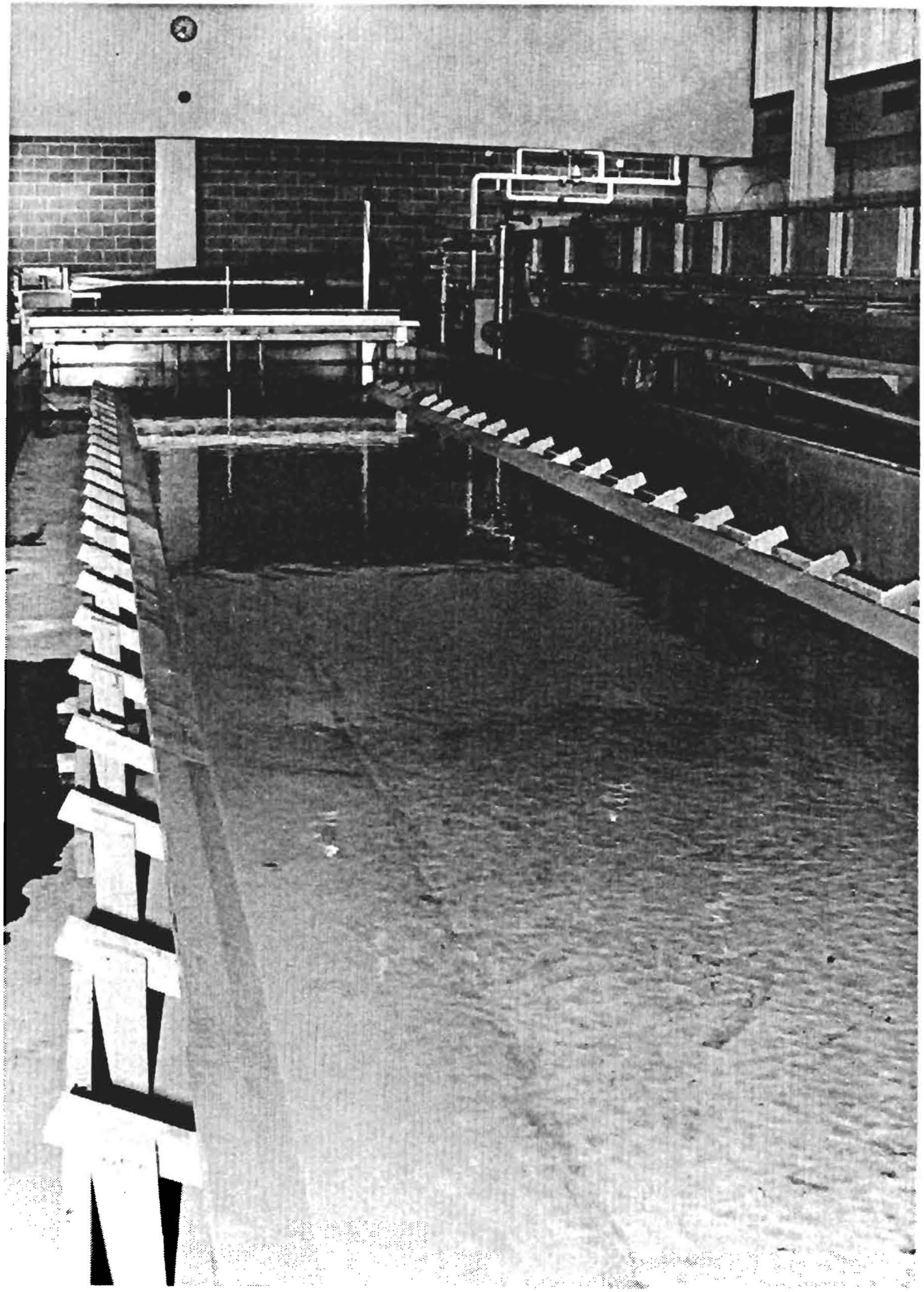

Fig. 13-Overall View of Flow Over 10-ft Weir Looking Downstream; Q=25,000 cfs; Tailwater Elevation=75 ft

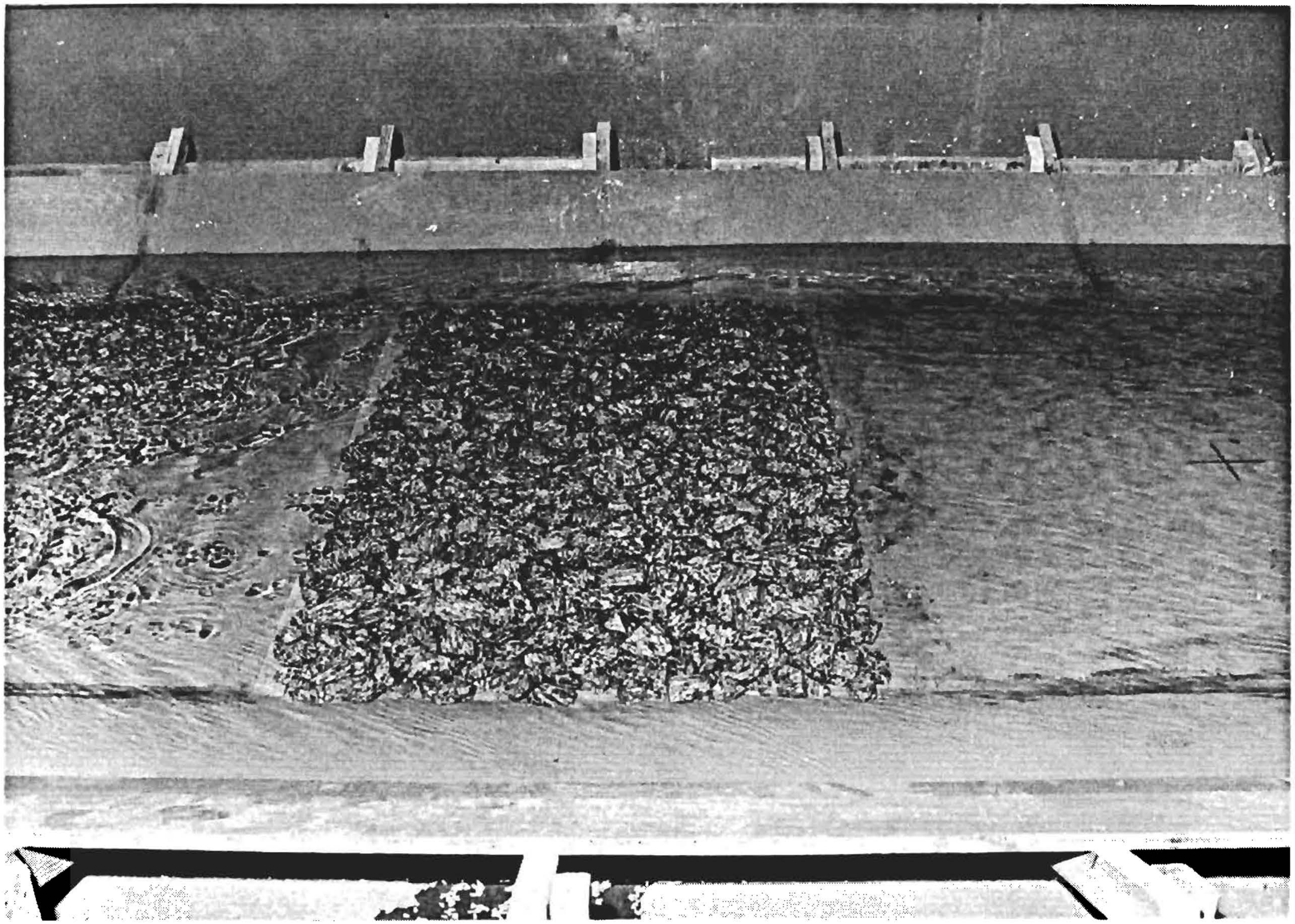

Fig. 14-Close-Up View of Flow (Right to Left) Over
10-ft Weir; Q=25,000 cfs; Tailwater Elevation=68 ft

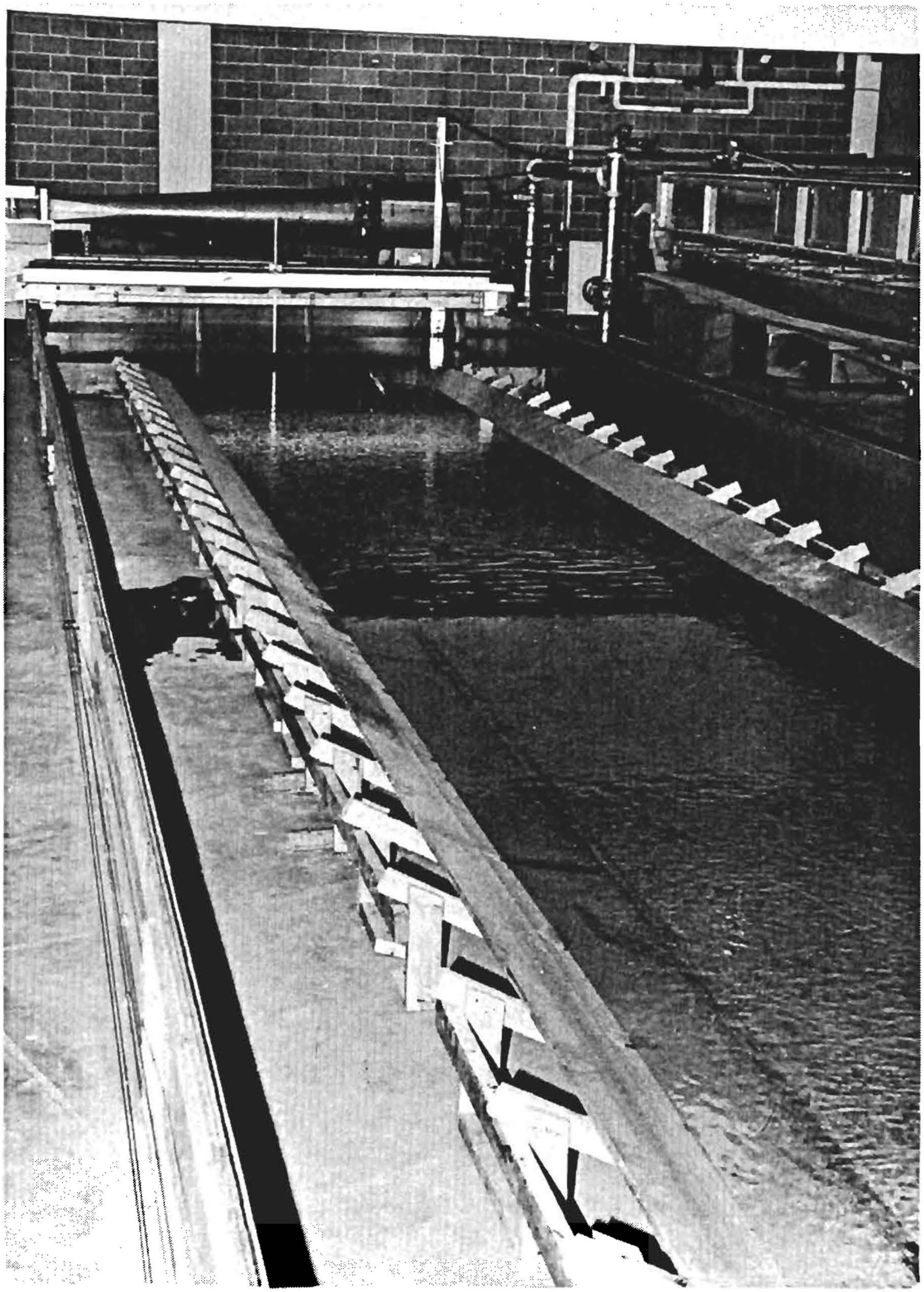

Fig. 15-Overall View of Flow Over 10-ft Weir Looking Downstream; Q=25,000 cfs; Tailwater Elevation=68 ft

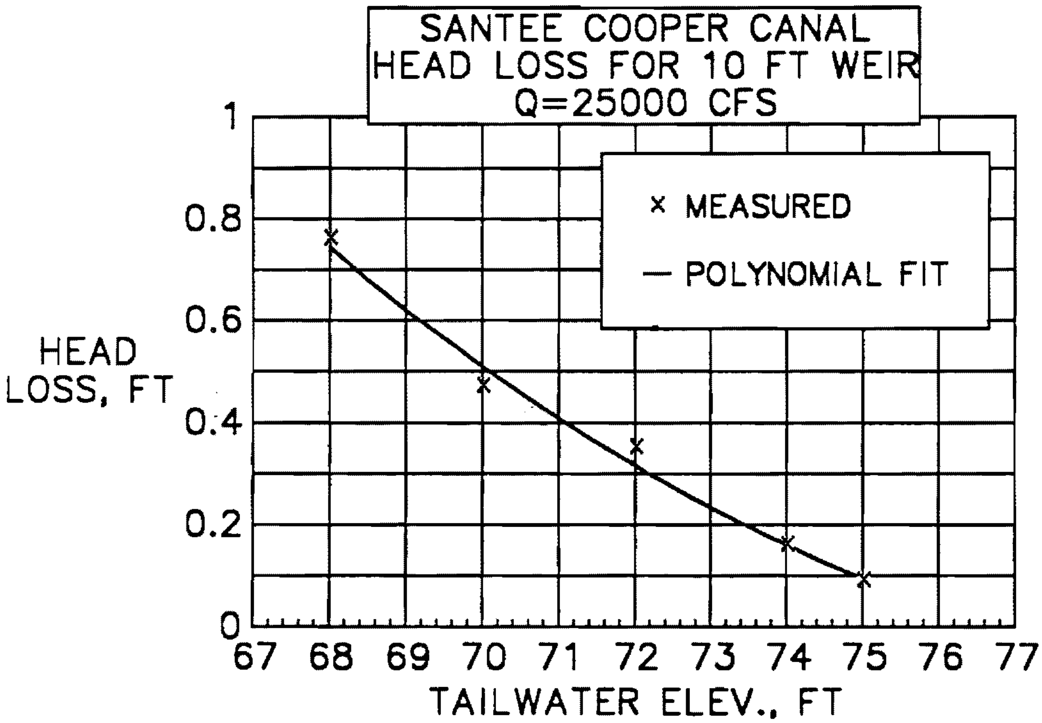

Fig. 16-Steady-State Head Losses for 10-ft Weir; Q=25,000 cfs

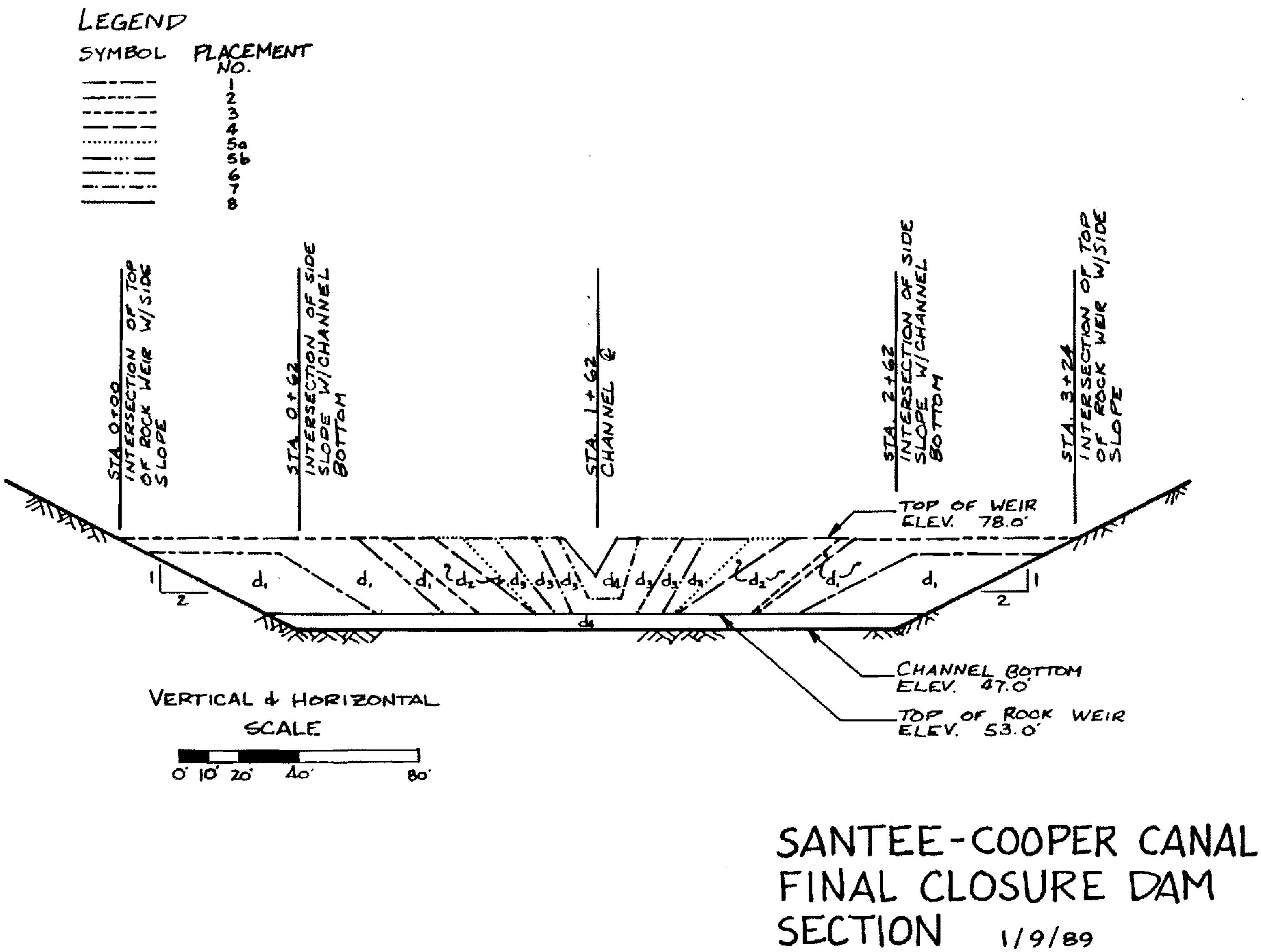

Fig. 17-Rock Size Zones for Each Closure Placement

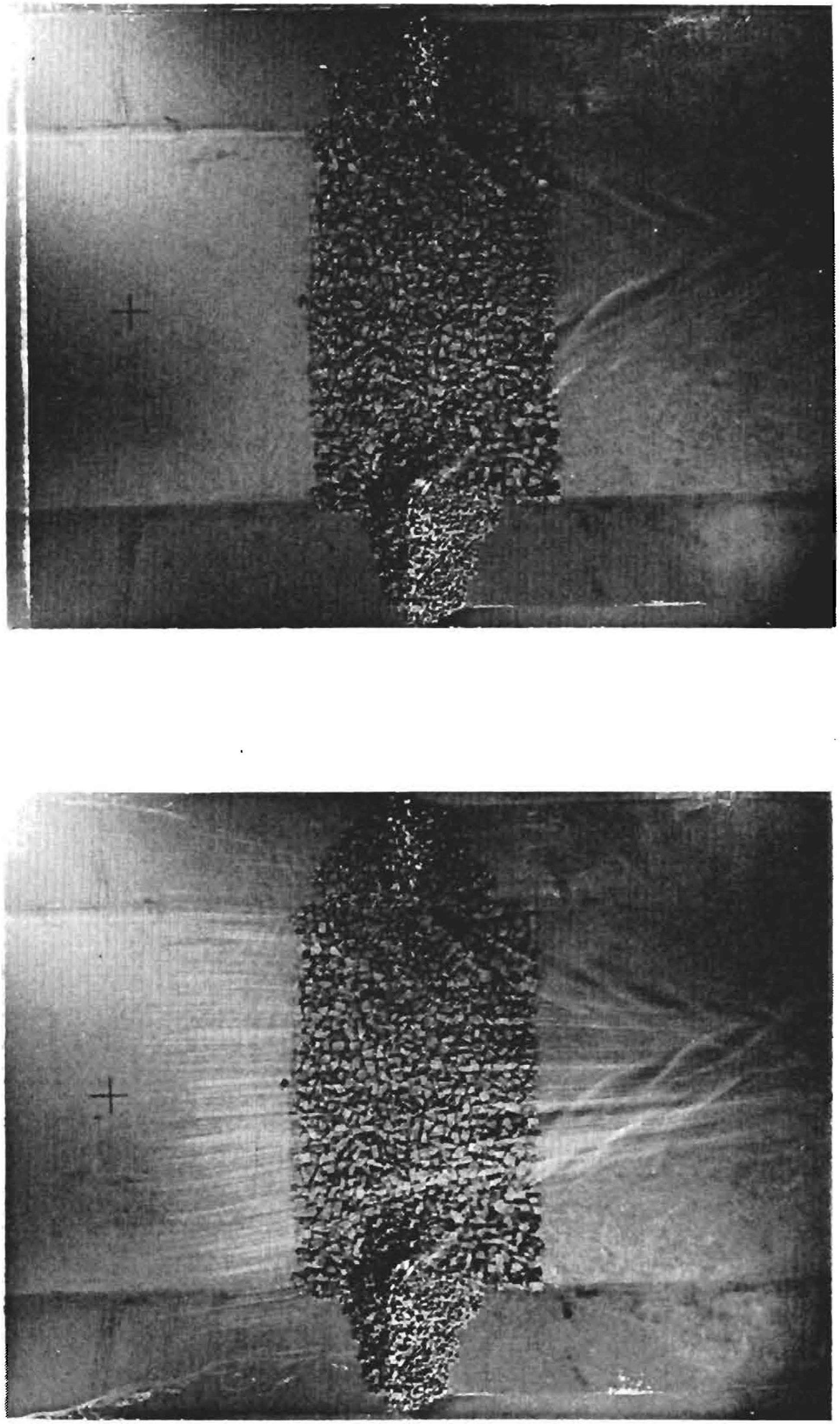

Fig. 18-Overhead View of Flow (Left to Right) Through Closure Constriction at End of Placement No. 1

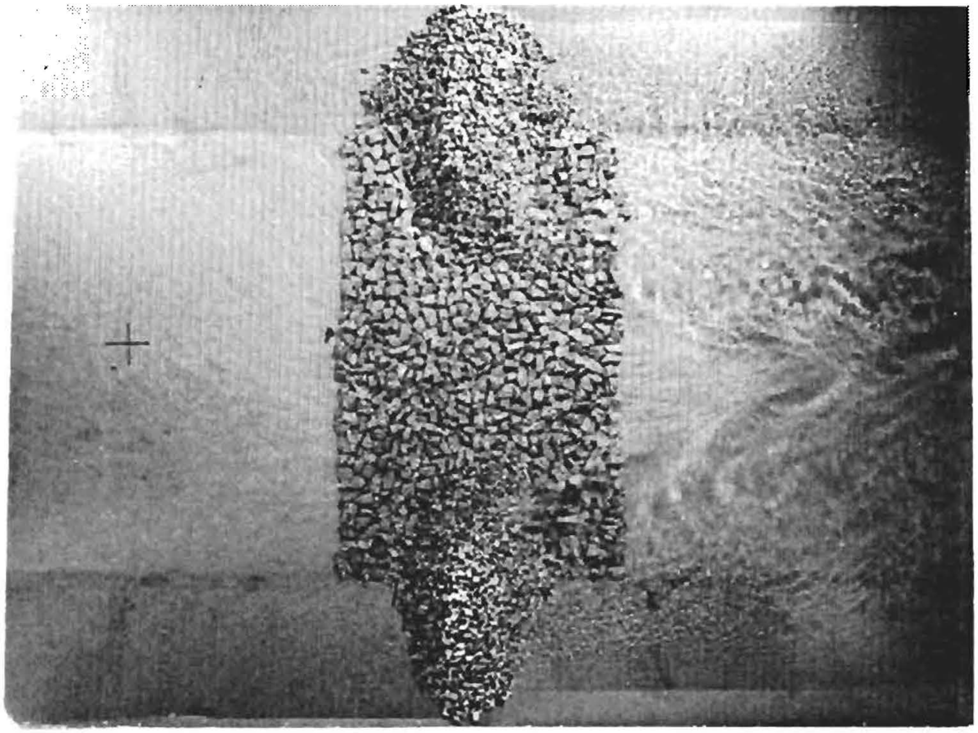

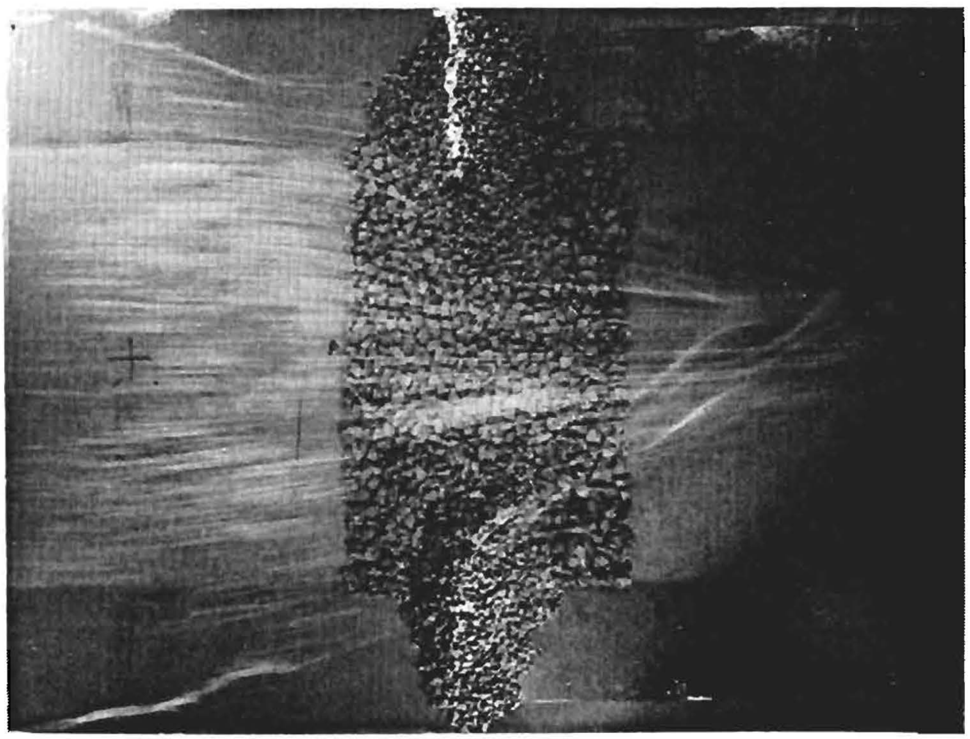

Fig. 19-Overhead View of Flow (Left to Right) Through Closure Constriction at End of Placement No. 2

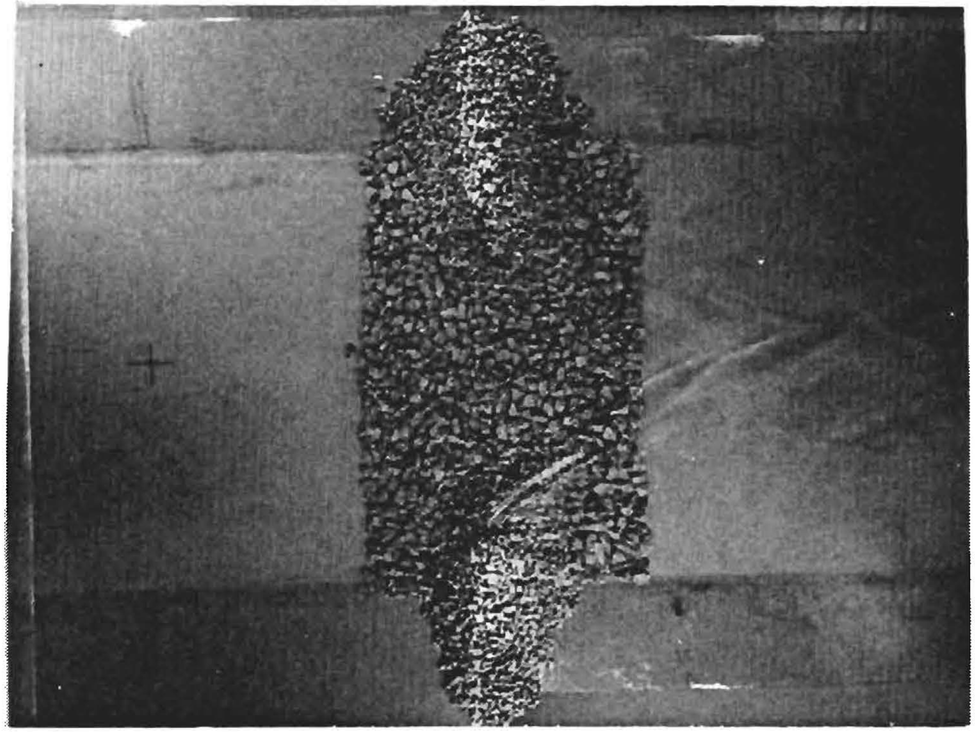

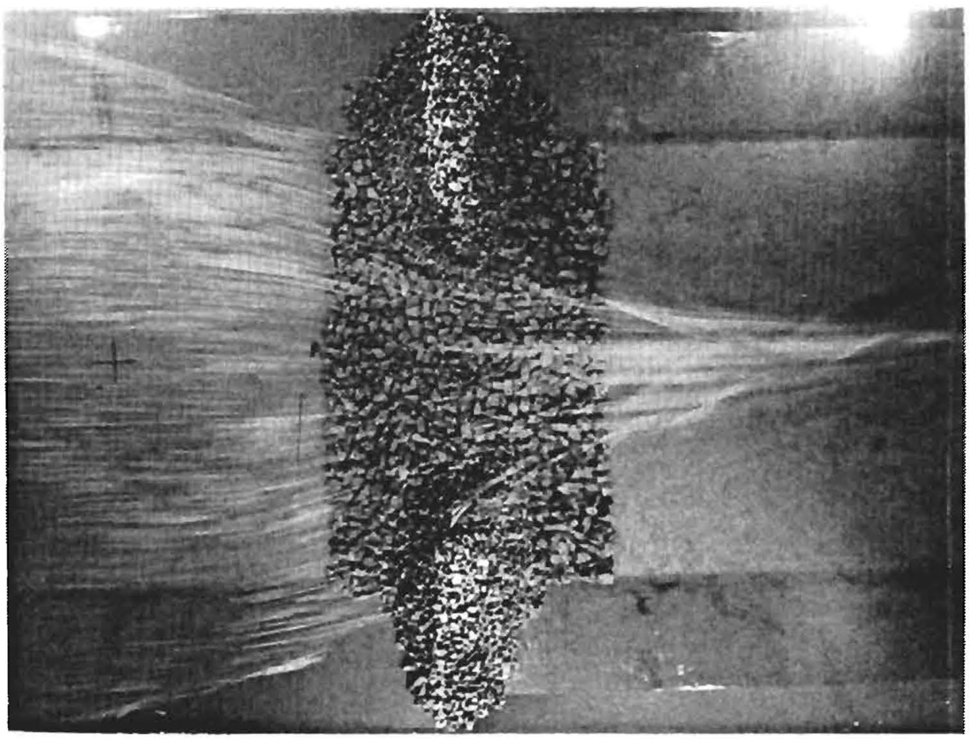

Fig. 20-Overhead View of Flow (Left to Right) Through Closure Constriction at End of Placement No. 3

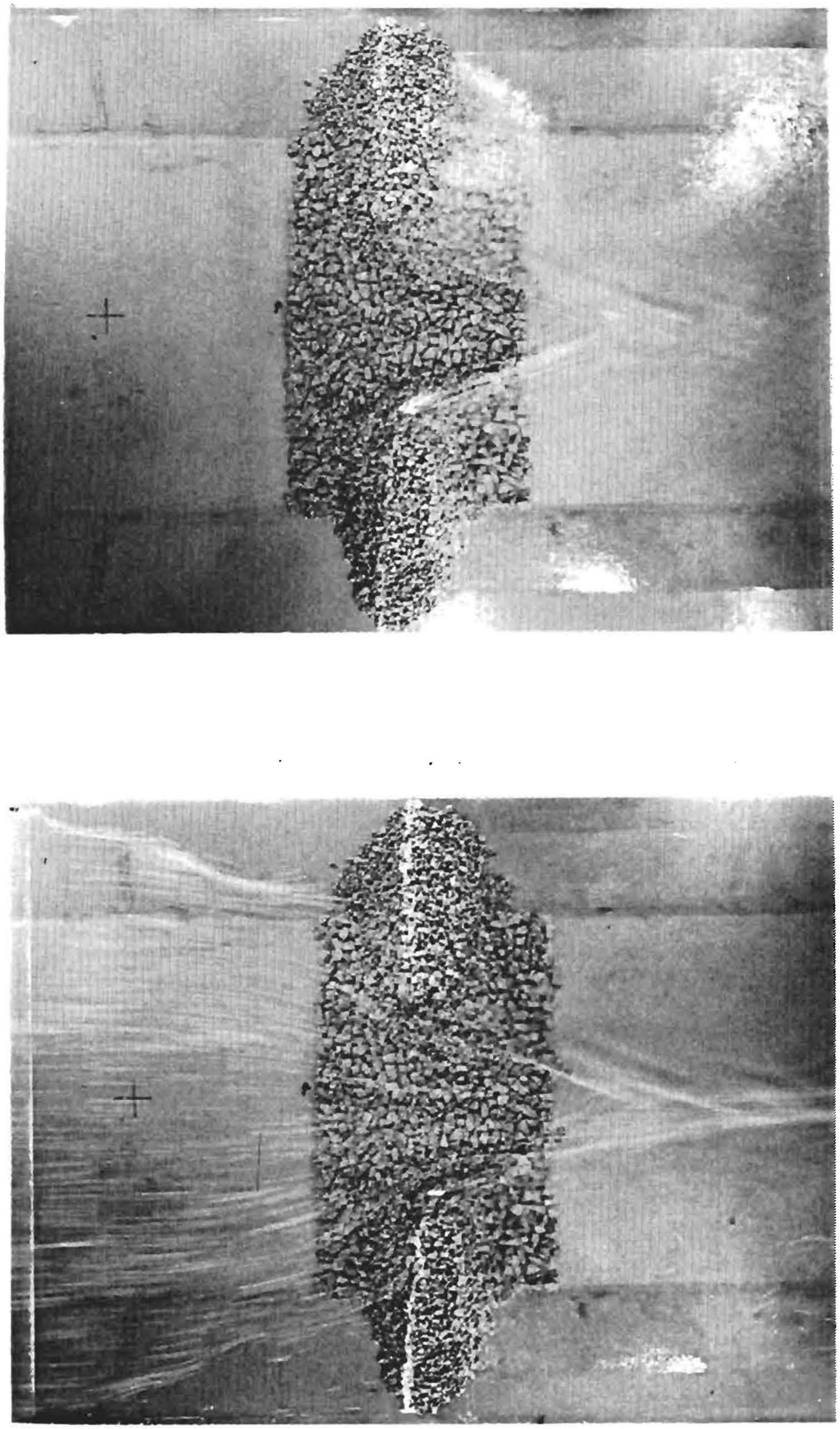

Fig. 21-Overhead View of Flow (Left to Right) Through Closure Constriction at End of Placement No. 4

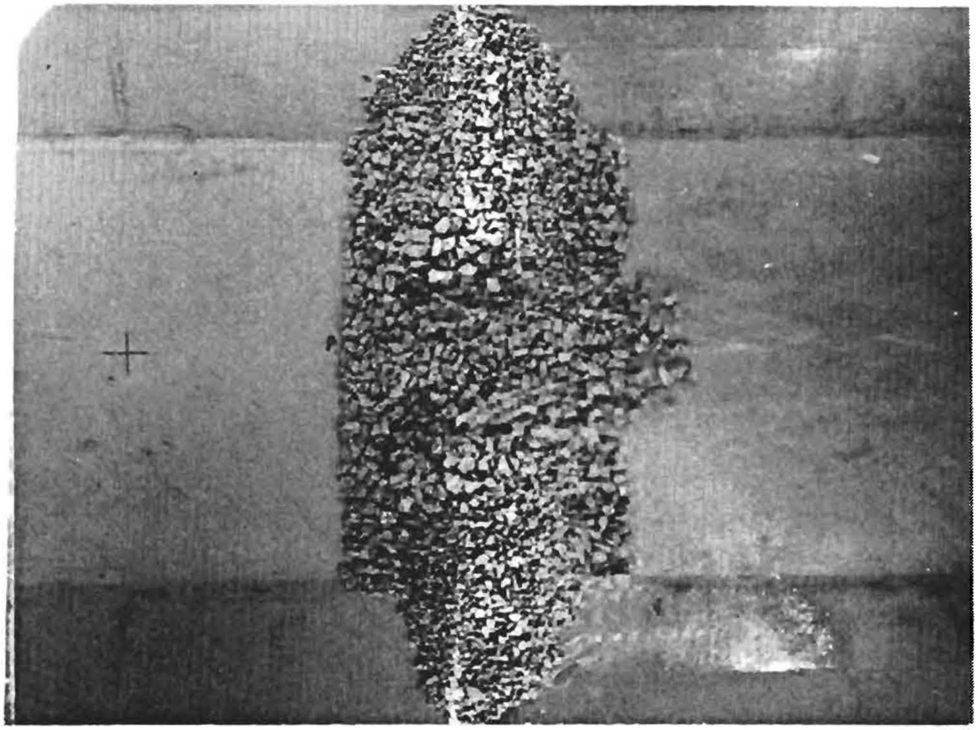

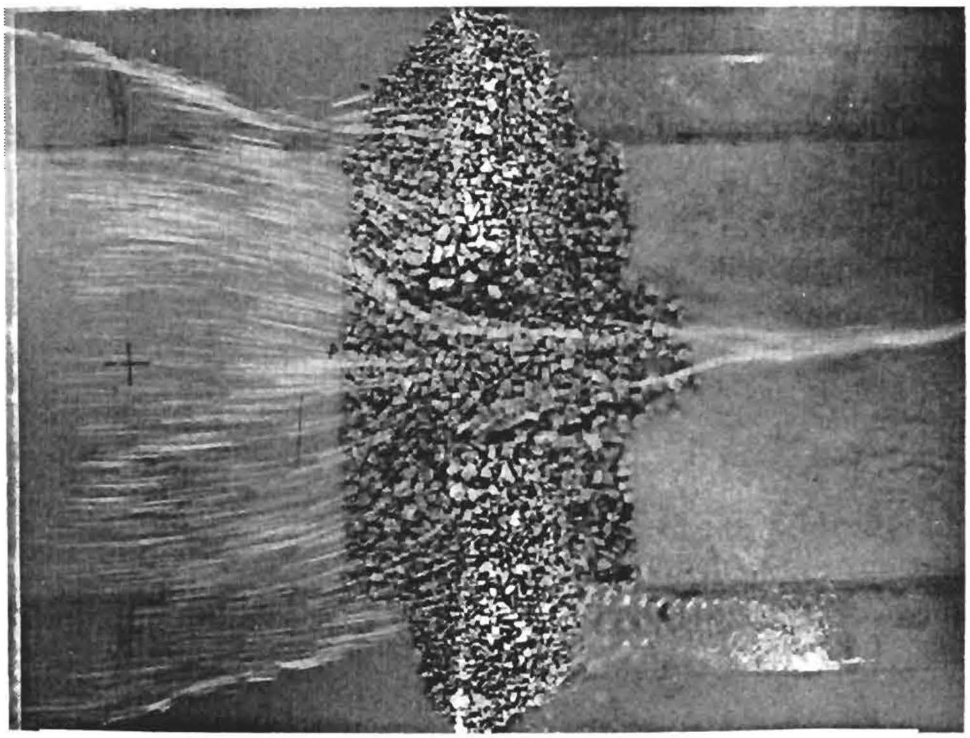

Fig. 22-Overhead View of Flow (Left to Right) Through Closure Constriction at End of Placement No. 5

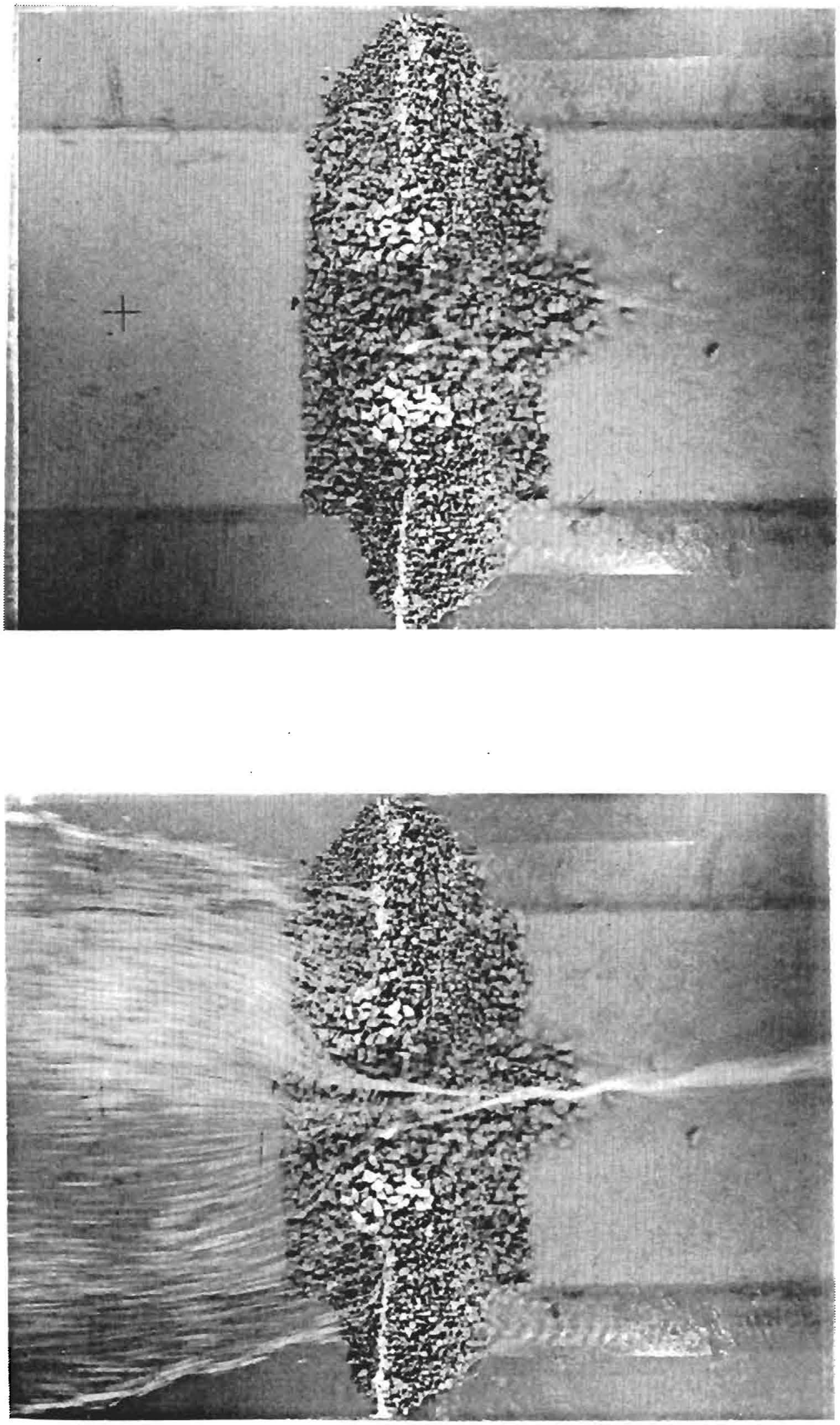

Fig. 23-Overhead View of Flow (Left to Right) Through Closure Constriction at End of Placement No. 6

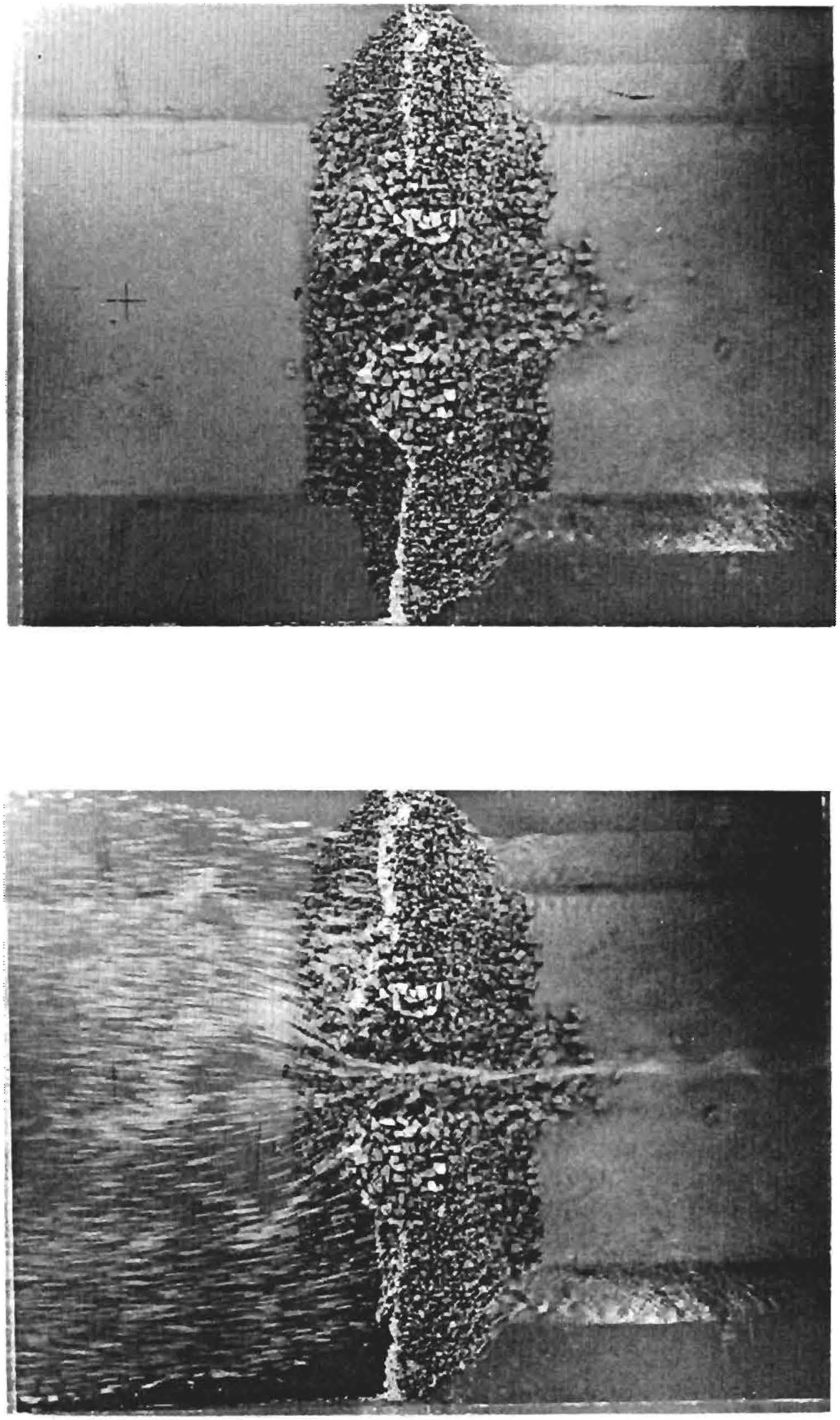

Fig. 24-Overhead View of Flow (Left to Right) Through Closure Constriction at End of Placement No. 7

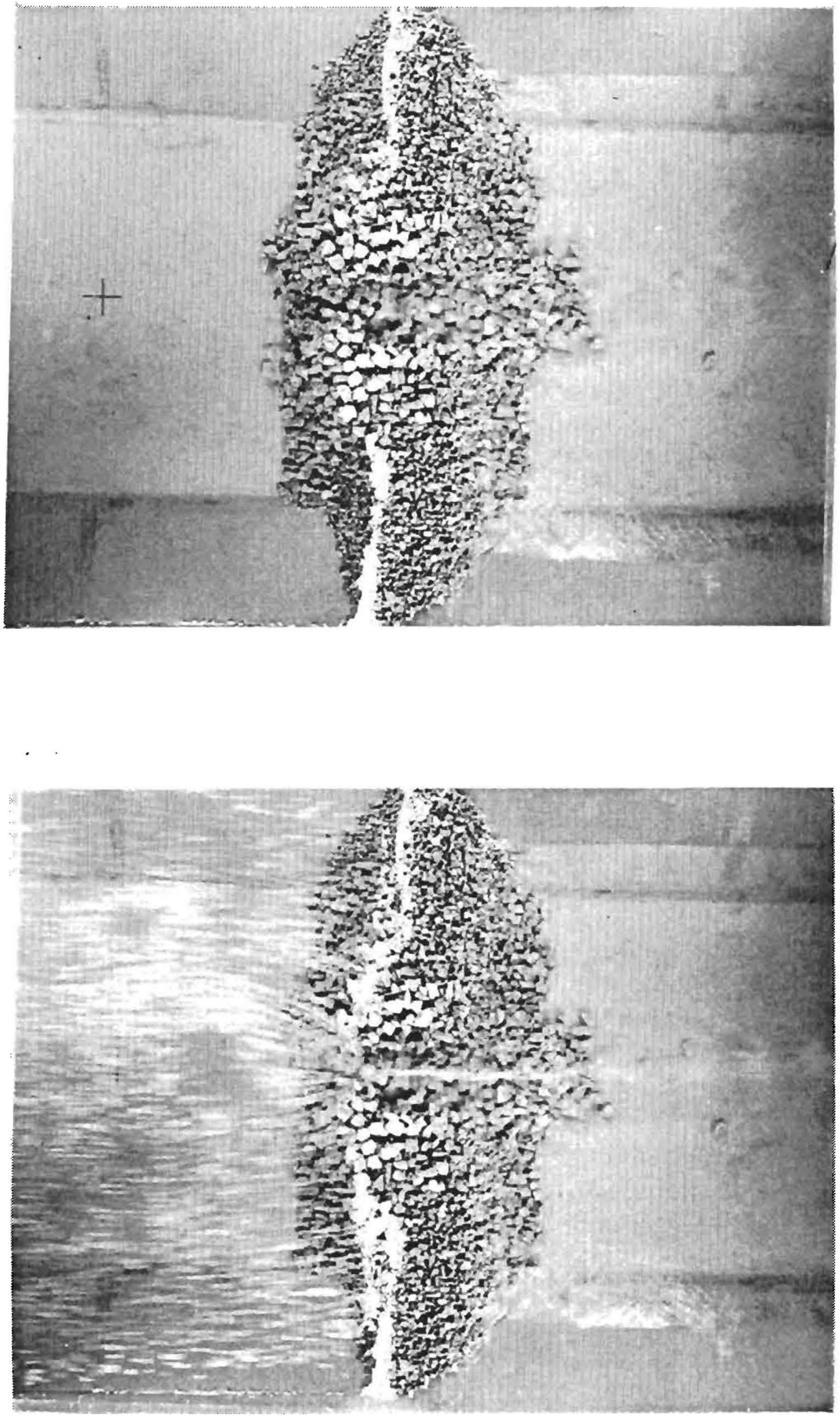

Fig. 25-Overhead View of Flow (Left to Right) Through Closure Constriction at End of Placement No. 8

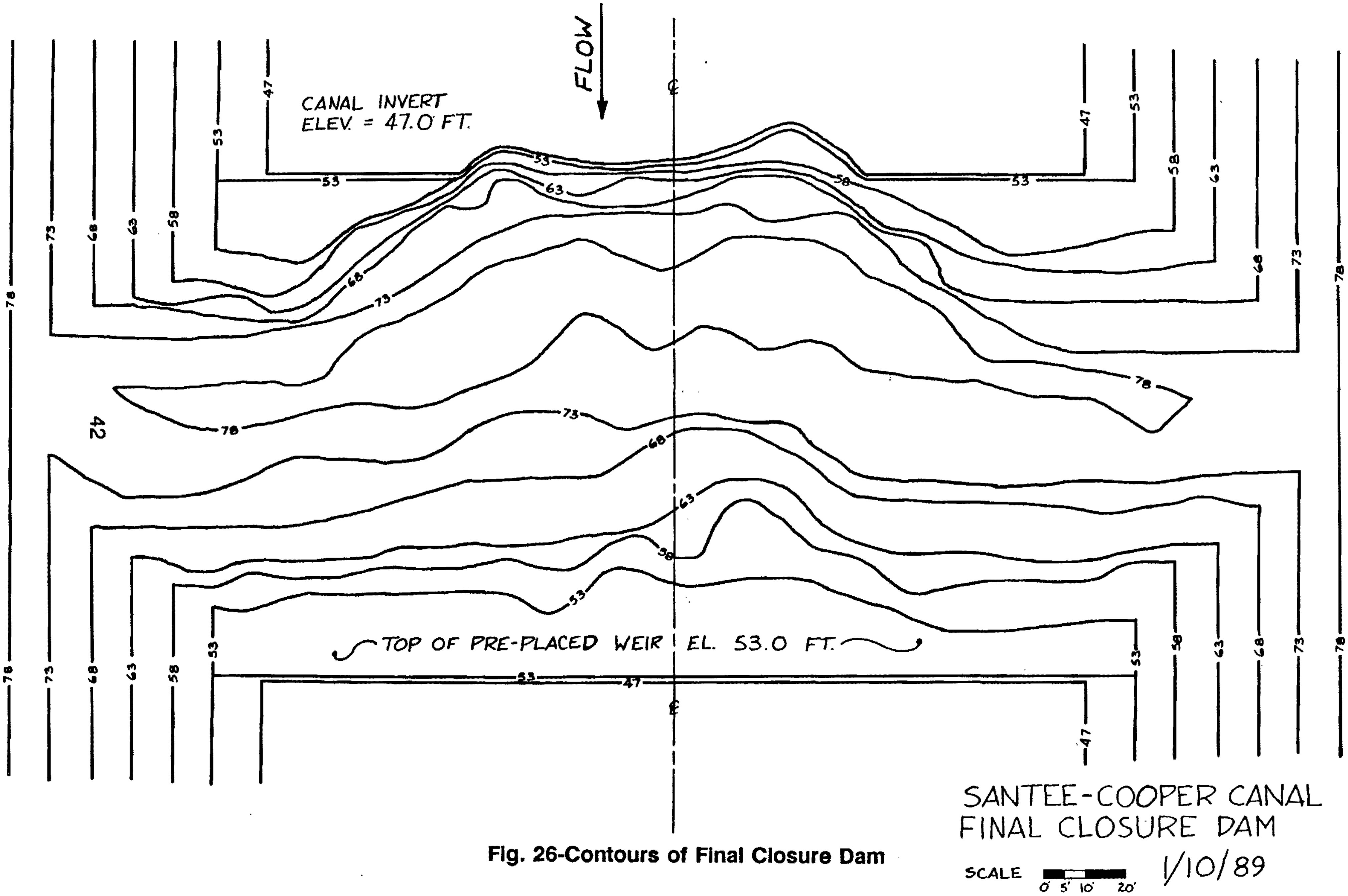

Fig. 26-Contours of Final Closure Dam

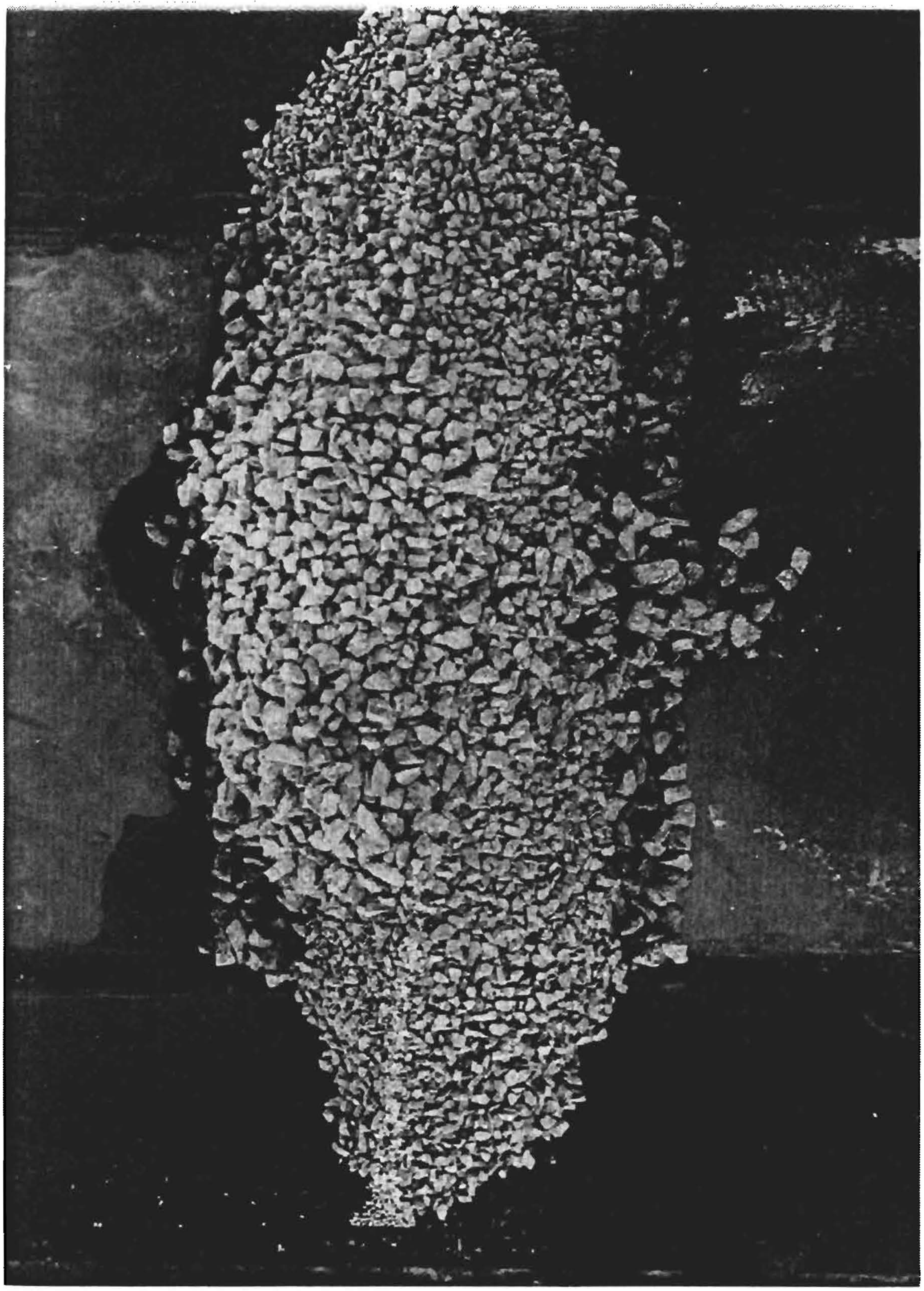

Fig. 27-Overhead View of Final Closure Dam
(Upstream on Left Side)